Irradiation Growth Modeling of Zirconium in Nuclear Reactors

Sang Il Choi

Department of Nuclear Engineering

Graduate School of UNIST

2014

Irradiation Growth Modeling of Zirconium in Nuclear Reactors

A thesis

submitted to the Graduate School of UNIST

in partial fulfillment of the

requirements for the degree of

Master of Science

Sang Il Choi

07. 15. 2014

Approved by

———————————————

Ji Hyun Kim

Irradiation Growth Modeling of Zirconium in Nuclear Reactors

Sang Il Choi

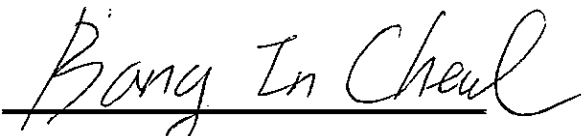This certifies that the thesis of Sang Il Choi is approved.

07. 15. 2014

Ji Hyun Kim

Dong Seong Sohn

In Cheol Bang

Abstract

Zirconium and zirconium alloys are extensively used as nuclear core material due to their excellent ability to withstand reactor conditions including corrosion and neutron irradiation. Despite their excellent properties as structure material, radiation-induced phenomena (growth, hardening, creep, and amorphization) are still main concerns at structure materials. Among them, irradiation growth is main concern in zirconium base alloy.

In nuclear reactor condition, main design criteria of zirconium alloys is corrosion. Therefore history of zirconium alloy development has been done to develop it which has better corrosion resistant properties. Representative zirconium alloy in nuclear society such as Zircaloy-1, Zircaloy-2, Zircaloy-4 and Zirlo are materials which show high corrosion resistant property. So far, irradiation growth was not main concern of nuclear plant safety criteria because of corrosion phenomenon. Therefore irradiation growth research is still insufficient compare with corrosion research filed.

Nowadays, however, commercial reactor life extension is needed and research reactor is received more neutron flux than commercial thing. Therefore, safety analysis of irradiated materials is become important. Irradiation growth combine with irradiation hardening could induce materials failure. Therefore this is the timing to analysis of irradiated materials.

So far, to recognize environment and material parameter effects on growth, extensive experiments have been done and some important experiments were completed. In the extensive research, to figure out the individual sink effects (grain boundary and dislocation loop and line, texture) on the growth mechanism, irradiation growth of single crystal experiments had been done. After single crystal growth data were analyzed, polycrystalline and zircaloy were also researched systemically. From these experiments, major parameter effect on irradiation growth was conformed. After growth experiment, specimen was analyzed by microstructure morphology such as sink density and size. From microstructure change, researcher could analyze irradiation growth mechanism. In 1980s, a lot of research had been done irradiated materials. Eventually, in rate of 1980s, research about irradiation growth, microstructure and growth theory are published.

However, recently, microstructure morphology change and fundamental parameter are updated and anisotropy diffusion difference concept was developed. Former research does not contain these developed. Recently theoretical modeling, which contain new developed concept, has been done in single modeling. However irradiation growth of polycrystalline and zircaloy do not developed. Therefore this research object is modeling of irradiation growth from single crystal to zircaloy.

To modeling of irradiation growth, in the literature study, microstructure change morphology and growth experiment were systemically reviewed by organization from single crystal to zircaloy. Also theoretical analysis, which conducted various authors are reviewed. At lastly, defect rate theory, which could explain microstructure change fundamentally, is reviewed for theoretical modeling.

In the results, based on the defect rete theory, improved theoretical modeling are suggested and growth results are presented from single to zircaloy. Before to growth modeling in research reactor, growth modeling are conducted at commercial reactor condition because there are more extensive research results are exist in commercial reactor condition. These results also conducted systemically form single to zircaloy for represent individual sink effect on growth. Individual parameters effects on irradiation growth are analyze by growth modeling results. Many metallurgical conditions eventually change the material parameters hence texture, grain size, dislocation density effect on growth are analyzed and also experimental conditions effect on growth are reviewed.

In case of single crystal and cold worked polycrystalline, the growth result show well agreement with experimental result. For the fundamental understanding of these case, the behavior of the defect flux and sink strength behavior are analyzed. From this analysis, it was clear that the growth modeling are well established. However, in case of annealed polycrystalline case, the results was not well matched with experimental results because in case of polycrystalline case, the sinks behavior are more complex than single and cold worked case.

Unfortunately, irradiation growth modeling of annealed polycrystalline was disagreement of experiment result. However, from the detail analysis in result and discussion, it was clear that limitation of the modeling and improvement direction. Therefore, in the future work, assumption of defect rate equation will be extended to cluster and grain boundary sink strength modeling will be conducted. Also irradiation growth equation will be modified to contain <c> axis shortening. Diffusion coefficient is most important parameter in the modeling result. Therefore, defect induced diffusion coefficient change also will be treated. This specific work will be done with MD simulation.

Contents

III

I.   Introduction

1.1 General background:

In nuclear power plants, zirconium and its alloys are used extensively to store nuclear core material due to their ability to withstand reactor conditions for long periods of time, including neutron irradiation. Specifically, zirconium alloy are used such as cladding, guide tube and grids in PWR and also used such as pressure tube in CANDU reactor, lastly in case of research reactor, zirconium alloy are used such as guide tube and reactor vessel. Despite their excellent properties as structure materials and significant manufacturing progress, radiation-induced phenomena (growth, hardening, creep, and amorphization) are still main concerns.

Irradiation growth is one of the most important phenomena which should be avoided in order to maintain structural integrity because irradiation growth is a dimensional change of materials without applied stress or volume change under irradiation to materials. Irradiation growth could make zirconium base component failure with radiation induced hardening [1].

Irradiation growth occurs only in anisotropic materials, because the defect diffusion coefficient is different between the basal plane and the prism plane [2], Self interstitial atom (SIA) shows much more this tendency, i.e., high diffusion coefficient in basal plane and low diffusion coefficient in prism plain [3-5].

Zirconium alloy is one of the most typical materials shows anisotropy properties. Therefore irradiation growth is most dominant phenomenon compare with other radiation induced phenomena in zirconium. However, so far, growth is not major considering parameter in manufacturing process. Therefore, there is a little theoretical data which can be used in cladding or guide tube manufacturing process for optimizing component structure properties.

However, recently, growth becomes important parameter for life extension and improved safety analysis. Furthermore, due to design or operating conditions, zirconium alloy are located in various radiation conditions. Reactors could be divided into two large groups, such as research reactors and commercial reactors. Commercial reactors are operated with relatively high temperatures and low fluence conditions compared with research reactors. However, research reactors receive a higher fluence than commercial reactors in the same period. Therefore, it is very important to analysis zirconium growth behavior in various environment by using theoretical modeling

1.2 The goal and scope of this study:

This chapter describes the research goal and development. For life extension and improved safety analysis of zirconium alloy in nuclear reactor condition, this paper aim to establishment of irradiation growth characteristic at given environment by establishing irradiation growth model.

Therefore in this paper, experimental database of irradiation growth are established and microstructure change by irradiation is characterized. From experimental database, irradiation growth mechanism are and various theoretical modeling are reviewed. After then, radiation induced damage and define defect flux behavior with sink in zirconium alloy are calculated by quantitatively. And then theoretical growth modeling was established. From the theoretical modeling, zirconium alloy component in nuclear reactor could be verified its safety integrity by FEM(ANSYS).

II.   Literature study

2.1 Radiation-induced dimensional change

Before to review irradiation growth specifically, it have to be understanding that various irradiation deformation phenomenon. There are three representative dimensional change of metal material by radiation. That is growth, swelling and creep. These dimensional changes are classified by volume and stress. Irradiation growth is volume conservative distortion without applied stress and swelling is the isotropic volume expansion without any applied stress. Creep is the volume conservative distortion by the applied stress.
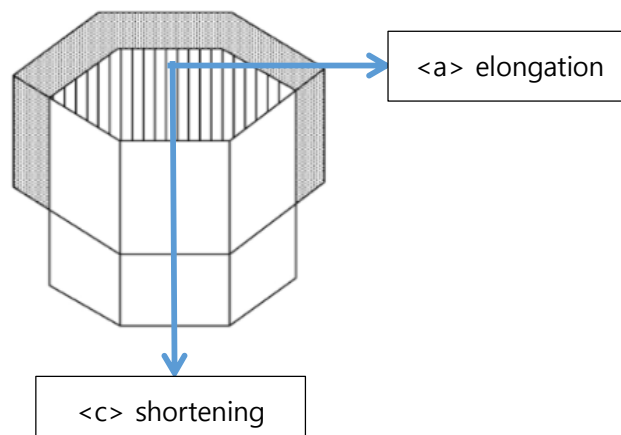

<a> elongation

<c> shortening

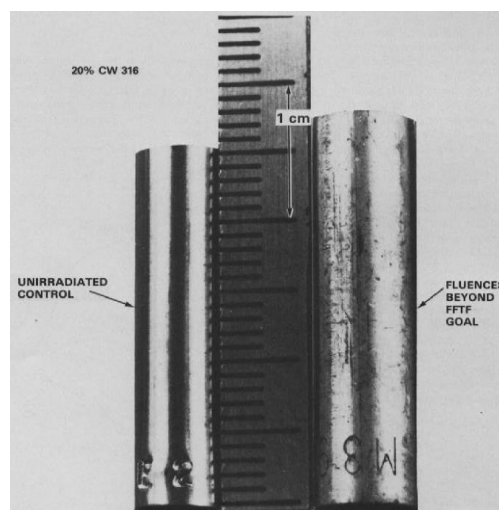Fig II.1 Schematic of the irradiation growth of H.C.P [6]

Fig II.2 The swelling which occurs in 20 % CW 316 SS [7]

All of the radiation induced phenomenon origin is defect flux behaviors in matrix. For these understanding, it has to be considered as a fundamental of radiation induced phenomenon mechanism. Radiation induced defect are consisted two type of SIA and vacancy. These defects in zirconium matrix show different behavior because of diffusion coefficient, activation energy, stress strain field and volume relaxation. Therefore, different behavior between SIA and vacancy induced unbalance defect flux behavior to the sink (dislocation line, dislocation loop, void, bubble, and precipitation). This concept is referred the diffusional anisotropy difference (DAD) by Woo [8]. Therefore understanding of bias is key factor to modeling of radiation induced dimensional change.

Fig II.3 shows the schematic of radiation damage phenomenon. Before the irradiation, defect concentration is very low. However, after irradiation, defect concentration dramatically increase with time. The white square is vacancy, black dot is SIA, blue square is vacancy cluster and red dot is SIA cluster by irradiation. Although almost radiation induced defect are annihilated by cascade relaxation and thermal recombination, small amount survived defect (1~2%) are generated sufficiently to change of microstructure. The decreasing rate of SIA concentration is faster than vacancy, which is shows in the left side figure that white square is many than black dot. This reason will explain in detail in next section. Therefore, SIA defect flux to sinks is reinforced by irradiation. After that, microstructure is changed by bias defect flux. The specific sink density are increased and then macro structure is changed.
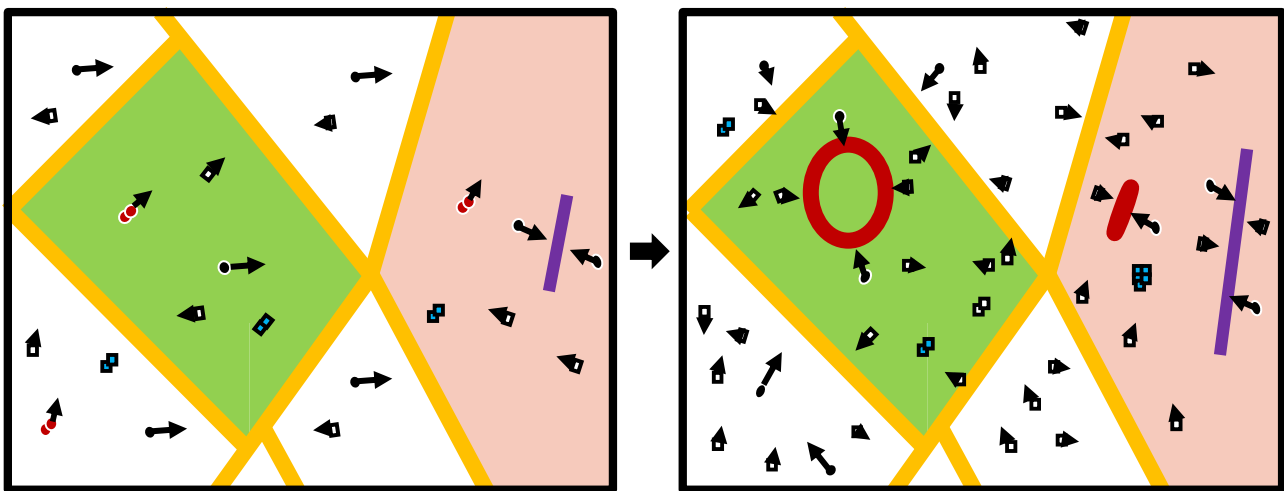

Fig II.3 Schematic of microstructure before & after irradiation

4

The difference of swelling and growth phenomena origin is based on the DAD concept and stacking fault energy. In case of swelling vacancy preferential sink which is developed in the form of three dimension morphology because of high stacking fault energy. In case of growth, vacancy preferential sink form two dimensional sink because of low stacking fault energy. Two dimensional sink do not occur volume changing hence zirconium volume conserved while irradiation, However, only with two dimensional sink could not make dimensional change. To induce irradiation growth, DAD concept also is needed because if two dimension sink is distributed isotropy, volume change do not occur. Two dimensional sink is distributed anisotropy because of the DAD concept.

For example, In case of isotropic cubic materials, edge dislocation is SIA preferential sink and grain boundary is natural sink because SIA diffusion coefficient much higher than vacancy that. And vacancy, which has no preferential sink, is developed by the form of void or disk. Therefore in the matrix, sinks are growth or generated and eventually micro – macro structure are changed. However, in case of non-cubic metal systems (hexagonal closed pack), such as zirconium metal, have hexagonal close pack systems. Therefore usual analysis for cubic system could not be used to fundamental understanding of radiation induced phenomenon in zirconium. DAD concept should be used for analysis defect flux to sink. From this concept, it showed that edge dislocation is no longer SIA preferential sink and grain boundary is no longer neutral sink. After bias concept are developed, truly theoretical radiation induced deformation models are developed.
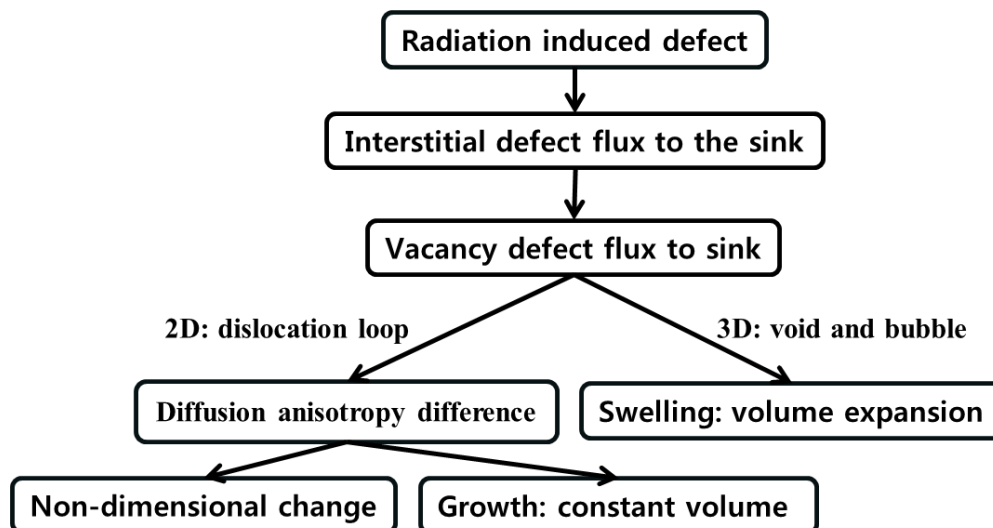

Fig II.4 Schematic of origin of swelling and growth

2.2 Radiation-induced growth

Radiation-induced growth indicates anisotropic dimensional change, i.e. expansion in the a-direction and contraction in the c-direction. Contrasted to swelling and creep, growth phenomenon is not accompanied by increasing volume and application of stress. Nevertheless, even in the absence of stress and volume expansion, growth is a complex phenomenon itself because it is dependent on many fundamental parameters. Therefore, we had to consider many material parameters and metallurgical conditions (texture, grain size, dislocation density, alloy component, heat treatment and cold work) and experimental conditions (fluence and temperature).

The history of irradiation growth of zirconium is started by Buckely in 1969 [9] and after that principle researched had been done by Fidleris [10] and Adamson [11]. In 1980s irradiation growth are researched in earnest by NRR programs. For the understanding of environment (fluence and temperature) effect on zirconium, three key parameters (temperature, fluenece and materials properties) are controlled by researchers. For instance, to recognize the degree of the importance of these parameter effects on growth, extensive experiments have been done and some important experiments were completed [12-22]. Specifically to figure out the sink effects (grain boundary and network dislocation induced by cold work) on the growth mechanism, researcher performed single crystal growth experiments. After these single crystal irradiation growth data were analyzed, polycrystalline zirconium and zircaloy were also researched systemically. And from these experiments, it was conformed that major parameter effect on irradiation growth. After experiment, sink morphology change are researched and mechanism was analyzed.

In recent years, several experiment of irradiation growth also had been done in the pressure tube part of CANDU reactor. However, unfortunately, these research did not include theoretical approach to analysis of sink effect [23-27].

2.2.1 Single crystal zirconium

Carpenter reviewed single crystal zirconium growth behavior [12, 13] by a Northern Research Laboratories (NRL) program as underlying the study of radiation-induced growth in zirconium and its alloys. Fig II.5 shows Carpenter's growth strain results at 553 K and fluence up to 7×10^{25} n/m^2. Zirconium metal could be divided two large groups based on the manufacturing process, iodide- and zone–refined. In the case of iodide growth strain results show three regions. First, the transient stage is observed to elongate along the a-axis rapidly, showing saturation growth strains are approximation 10^{-4} at fluences below 2.5×10^{25} n/m^2. Growth remains in the stationary stage until a fluence of 3×10^{25} n/m^2. After stationary stage growth breakaway, accelerated growth is observed. At a fluence of 7×10^{25} n/m^2, the growth strain reaches 5.25×10^{-4}.

In the case of zone-refined zirconium, the transient stage region is larger than that of iodide and increases almost linearly at a rate of 4.5×10^{-30} m^2/n up to 1.5×10^{-4} growth at a fluence up to 1.5×10^{25} n/m^2. Reaching a strain of 3.25×10^{-4} at $\sim 5.9 \times 10^{25}$ m^2/n. However, in the stationary and breakaway stages, growth strains shown are hard to distinguish from iodide-refined. In both cases of iodide- and zone-refined zirconium, the c-axis growth could not be identified in this fluence range.
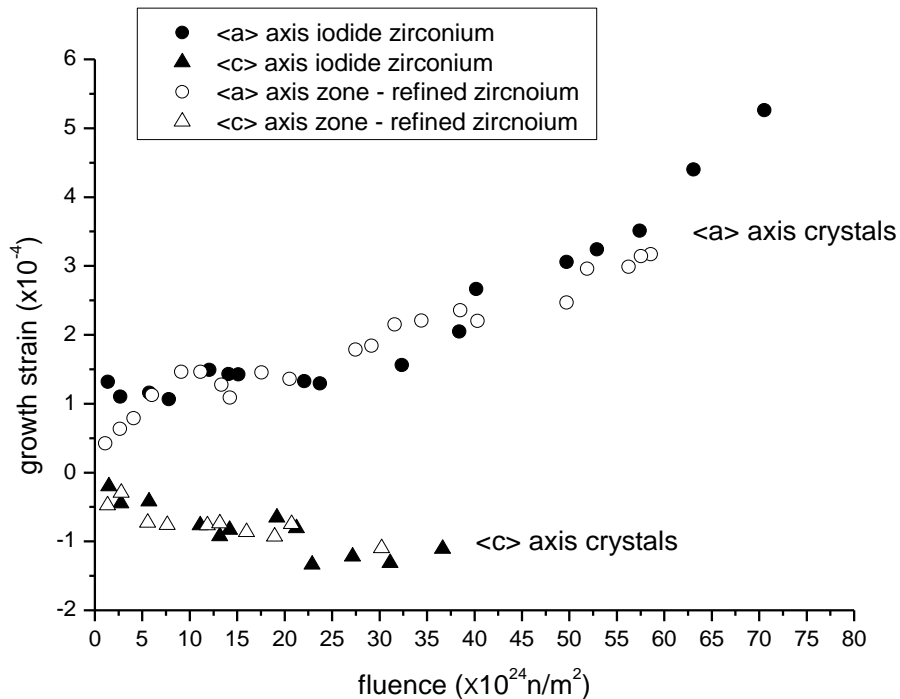
Fig II.5 Irradiation growth strain at 553K in annealed iodide and zone-refined zirconium single crystals [13]

2.2.2 Polycrystalline zirconium

In order to understand the element effect on the zircaloy growth mechanism, another pioneering group using polycrystalline zirconium specimens also researched growth phenomena in a NRL program. Polycrystalline growth behavior research is meaningful because it could reveal the growth dependence of an alloy's individual elements. Rogerson's growth strain results for iodide zirconium in the temperature 353 and 553 K are illustrated in Fig II.6 and Fig II.7 [16].

Specimens tested had different grain sizes: 5 μm, 40 μm, and 75 μm. The intent was to figure out the growth dependency on grain size and different textures. Annealed, polycrystalline, iodide-refined zirconium shows a linear increase in texture-dependent growth strain until 6×10^{24} n/m^2 at 353 K. In these figures, texture is expressed by F_d which is the resolved fraction of basal poles in any given direction. More detail information on F_d will be given in the later section regarding radiation-induced growth modeling. After saturation, growth strain is discernible. However, the grain size has little effect on growth rate. Moreover, at 553 K, the same material shows a higher dependency on grain size.
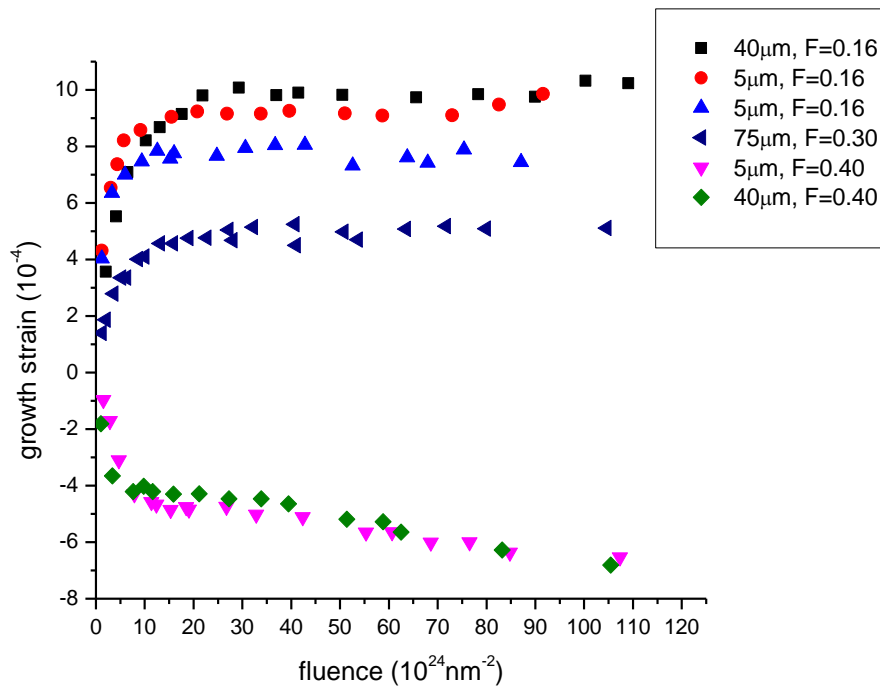
Fig II.6 Irradiation growth strain at 353 K in annealed polycrystalline iodide zirconium [16]
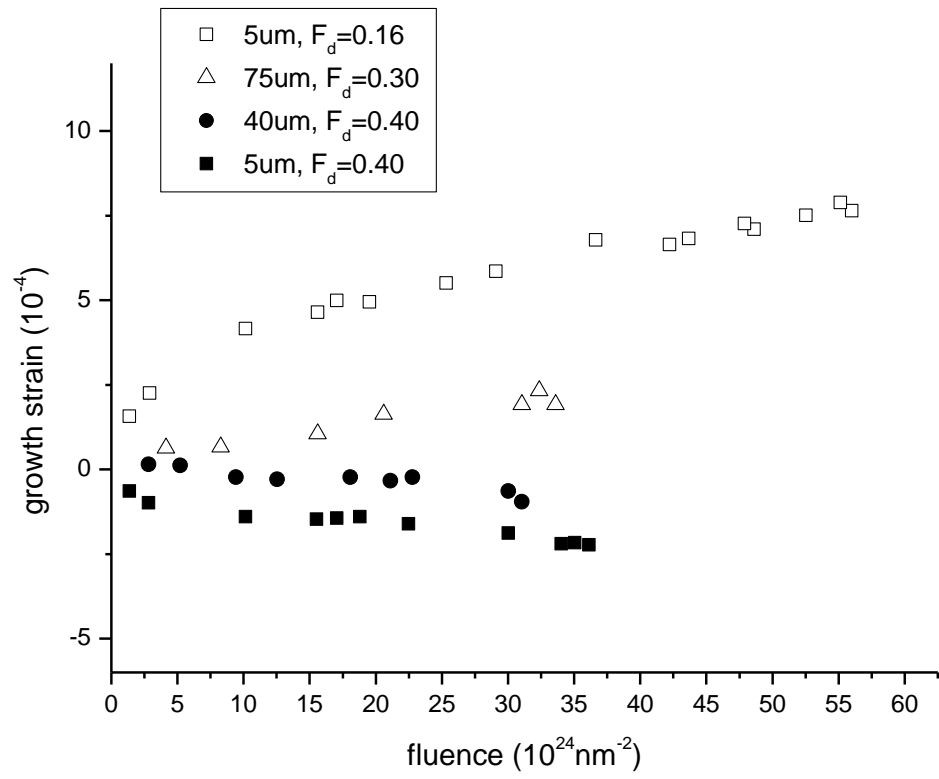
Fig II.7 Irradiation growth strain at 553 K in annealed polycrystalline iodide zirconium [16]

2.2.3 Zircaloy-2 and Zircaloy-4

Before high fluence facilities were built, zircaloy was researched with low fluence for practical applications. Adamson is a pioneer in the area of zircaloy growth. Adamson adopted traditional approaches making use of three key parameters: material properties, fluence, and temperature to assess growth phenomena [11]. Experiments were completed at a reactor temperature of 555 K and a fluence up to 3.5×10^{25} n/m^2. To observe growth dependency on the cold work parameter, the experiment was controlled such that specimens tested had similar texture and irradiation conditions. In case of annealed zircaloy-4, growth strain saturated at fluence near 1.0×10^{25} n/m^2, whilst 78% cold work zircaloy-4 showed an almost linear increase with fluence, as shown in Fig II.8. However, at fluence below about 0.2×10^{25} n/m^2, the effect of cold work parameters on growth dependency was negligible.
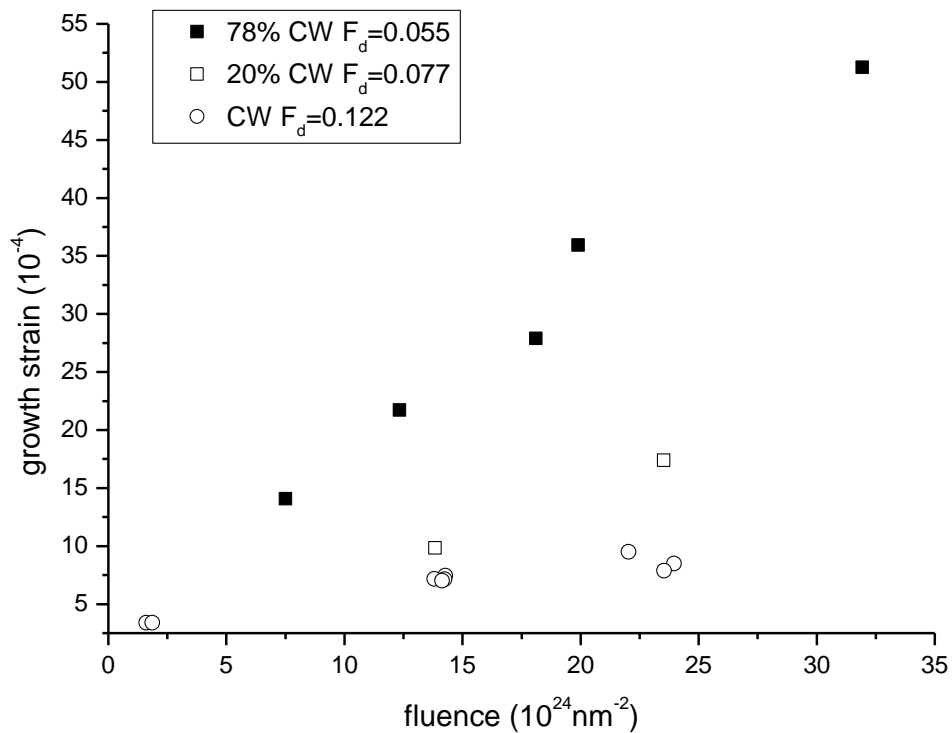
Fig II.8 Irradiation growth at 555 K in cold worked zircaloy-4 [11]

Fig II.9 represents the temperature and texture parameters' influence on radiation growth in annealed zirconium. For an f-factor around 0.1, growth strain is shown to be increasing with fluence up to 1.0×10^{25} n/m^2, but after the linear growth range, strain shows a tendency to saturate at 523 K. In the case of an f-factor around 0.33, relatively low growth strain is shown, as compared with other f-factor values. This is likely because texture is randomly distributed. Growth strain dependency on f-factors is observed more clearly at lower temperatures (<339 K). For fluence below about 0.5×10^{24} n/m^2, the growth rate dependency on the f-factor does not effected by temperature.
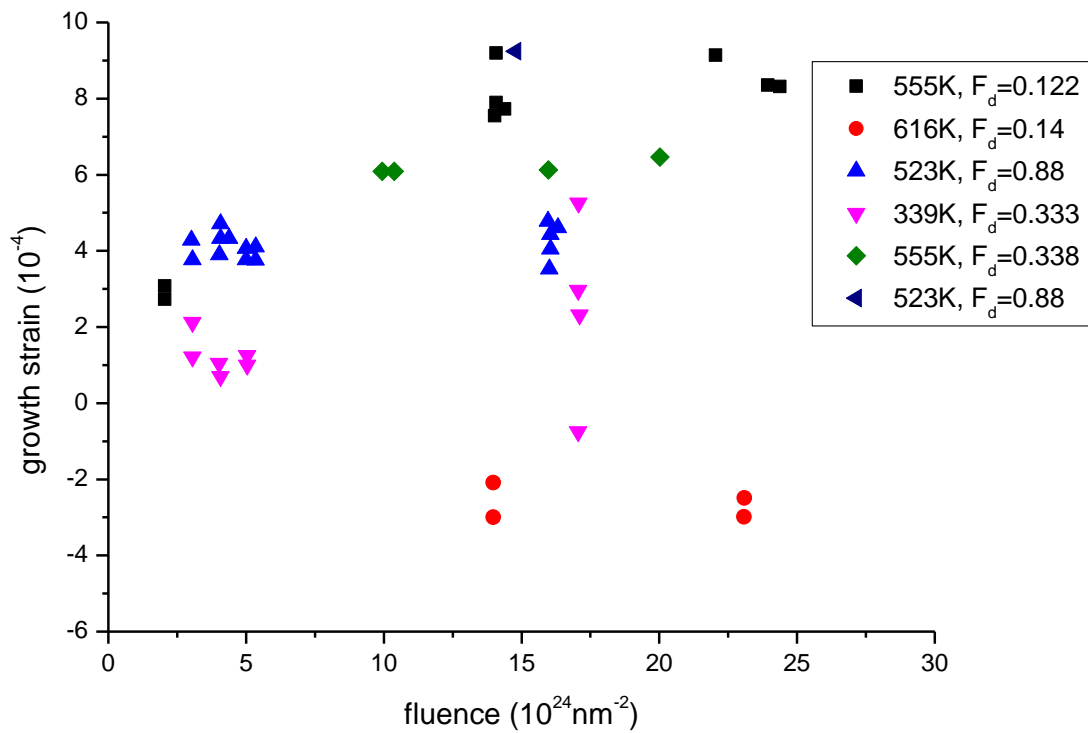
Fig II.9 Irradiation growth strain in recrystallized zircaloy-2 and 4 [11]

In the case of high fluence regions, zircaloy growth behavior was also analyzed, and researcher confirmed the influences of cold work and temperature dependency on growth. Annealed zircaloy-2 was used as a control group [15, 19]. Fig. 8 shows growth strain at 353 and 553 K and fluences up to 1.7×10^{27} n/m^2. At low temperatures, zircaoy-2 is rapidly saturated at a low fluence of 0.5×10^{24} n/m^2, whilst at 553 K, initial transient growth was relatively slow. However, after the transient stage, high temperatures show much greater growth strain. The growth behavior of 25% cold work zircaloy shows breakaway range and higher growth strain than annealed zircaloy-2. Annealed zircaloy at 353 K shows re-saturation at a fluence of 4×10^{25} n/m^2.
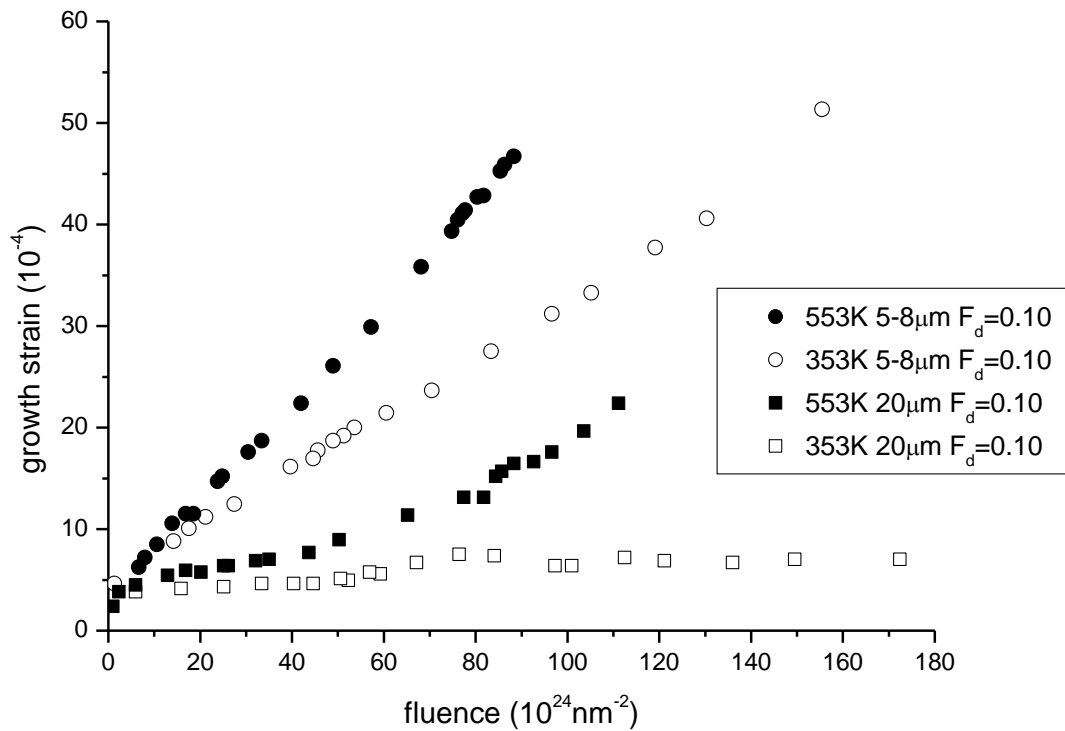
Fig II.10 Irradiation growth strain at 353 and 553 K in annealed and 25% cold-worked zircaloy-2

[16]

2.3 Radiation-induced microstructure change

As reviewed in previous chapter, extensive experiment has been conducted to evaluate growth behavior. Therefore, microstructure analysis are conducted for the quantitative analysis. From this research, three key parameters (fluence, temperature and materials variable) has explained quantitatively about their influence on irradiation growth behavior [10-15].

Before to analysis of microstructure, it should be understanding that mechanism of radiation induced microstructure change of zirconium. Simply explain about microstructure change, before the material is subjected to neutron irradiation, a certain amount of defects already exist, but many and more defect is formed upon neutron bombardment. In the case of zirconium and its alloys, stacking fault energy are small therefore two dimensional change are occurred. Defects are developed <a> dislocation loop and the <c> dislocation loop, which is characterized by Burgers vector.

Therefore, dislocations are used conceptually to analyze hardening and growth in zirconium and its alloys. Because zirconium have low stacking fault energies, In the initial stages of nuclear industry when irradiation growth phenomenon was firstly discover, extensive surveying had been done to revealed the nature of radiation-induced dislocation [11-26]. The dislocation loop is experimentally characterized by geometry, Burgers vector, size, and the proportion of vacancy and SIA loops.

However, in the 1980s, there was some discrepancies between radiation-induced growth phenomena and growth prediction models which is based on qualitative mechanism. Vacancy dislocation loop was appear in prism plane by microstructure analysis however in theoretical work vacancy loop in prism plane could not explain. Microstructure is fundamental to macro-scale behavior, hence, it was believed that understanding the correlation between microstructure and macrostructure can explain radiation-induced growth uncertainties and discrepancies. Therefore more extensive research about zirconium microstructure had been done in end of 1980s batter than other time.

2.3.1 <a> type dislocation loops

By the end of 1970s, numerous researchers had established typical dislocation characteristics in zirconium and zircaloy [11-26]. Dislocation loop is experimentally characterized by geometry, Burgers vector, size, and proportion of vacancy and SIA loops. Experimental results showed that all zirconium defects have the same Burgers vector $\vec{b}$ = 1/3 <1 1 2 0> and the same habit plain on (1 0 $\bar{1}$ 0) [11-12]. Temperature effects on dislocation consist of a decreased density and an increased loop size with temperature increase. Vacancy loop geometry shows circular shape with loop size less than 40 nm, but an elliptical shape with loop size larger than 40 nm. Interstitial cases tend to show a circular shape regardless of temperature.

Northwood *et al.* [13-15], who pioneered research in radiation damage in zircaloy-2, also examined zirconium metals. In these results, zircaloy-2 displays characteristics of dislocation similar to zirconium metal, in that both vacancy and SIA dislocation loops have Burgers vector $\vec{b}$ = 1/3 <1 1 2 0>, situated in the prismatic planes.

The influence of temperature on zircaloy also shows the same tendencies as zirconium metal in Northwood's papers, in that the loop density decreases and the loop size increases with increasing temperature. At 623 K, observed dislocations indicating a mean loop diameter between 8 nm and 10 nm and a loop density between 8.0×10^{21} n/m^2 and 5.0×10^{22} n/m^2, but a higher temperature at 673 K shows a mean loop diameter between 16 nm and 23 nm and a loop density between 4.0×10^{21} n/m^2 and 2.0×10^{22} n/m^2. Above 873 K, no radiation damage was observed [16]. At higher temperature, the irradiation-induced defects are generally annealed out by relaxation because the internal energy in material is sufficiently high for atom to move in normal lattice site.

The proportion of vacancy and SIA loops was also examined. At 623 K, the ratio of SIA and vacancy was balanced at 50%; however, with increasing temperature (until 673 K), the vacancy loop proportion increased to about 70%. At higher temperatures (>673 K), the proportion of vacancy loops drops to 20%. For lower temperatures (<573 K), the SIA loop type is dominant.

The effect of fluence is also conserved at constant temperature; before <c> component dislocation loops are observed, dislocation density increases rapidly with increasing fluence [16]. <a> type dislocation loops density tend to be saturated in fluence range of $1–2 \times 10^{24}$ n/m^2 at 573 K. Fig. 1 shows typical characteristics of <a> type dislocation loops.

Parameters such as dislocation size and density show a tendency of being proportional or inversely proportional based on conditions (temperature and fluence). However, <a> dislocation also shows common characteristics in that all loops have a Burgers vector $\vec{b} = 1/3 <1\ 1\ 2\ 0>$, which is parallel to the a-axis and habit on the prismatic planes $(1\ 0\ \bar{1}\ 0)$. Moreover, these types of loops are observed to coexist between vacancy and SIA types in the prism plain.
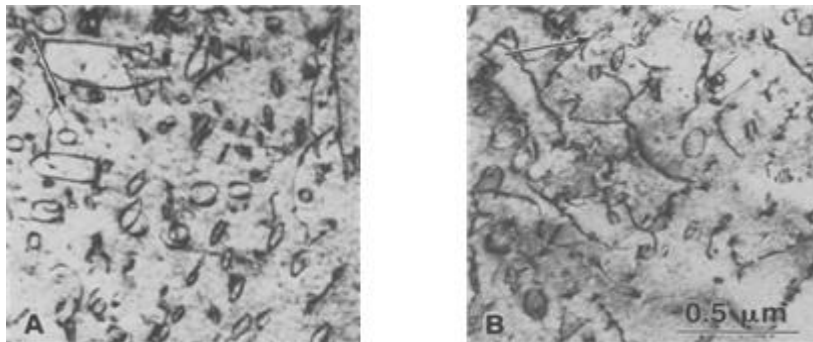

Fig II.11 Irradiation growth strain at 353 and 553 K in annealed and 25% cold-worked zircaloy-2 [28]

2.3.2 <c> type dislocation loops

Historically, <c> type dislocation is considered a major factor of growth breakaway phenomena [17]. Therefore, extensive surveying has been done to reveal the connection between <c> dislocation and growth. In the early stages of nuclear industry, there was no experimental evidence of the existence of <c> component dislocation loops due to the dearth of techniques to observe the c-type dislocation loop. In 1975, Bell and Adamson began to figure out the <c> component loop by using "corduroy structure," a term Bell coined [18]. Alternating bands of light/dark contrast seen under imaging conditions would reveal c-component dislocations of radiation damage.

<c> component dislocations are revealed by this technique [19]. These efforts revealed a <c> dislocation loop characteristic; that <c> loops are lying in the (0 0 0 1) plane and the Burgers vector is $\vec{b}$ = 1/2 <0 0 0 1> or $\vec{b}$ = 1/6 <2 0 $\bar{2}$ 3> along the c-axis. The loop type was observed to be only vacancy [20].

Holt and Gilbert [21] used high fluence (8.6×10^{25} n/m^2) in order to reveal <c> component dislocation loop characteristics between 553 and 584 K. Zircaloy-2 and zircaloy-4 irradiated with fluence below 3.0×10^{25} n/m^2 show only <a> dislocation and <c> component loops do not exist. However, for specimens irradiated at greater than 3.0×10^{25} n/m^2, <c> loops appeared. In Holt's research, <c> loops showed another special characteristic: high density <c> component dislocation associates with second-phase particles.

The correlation between <c> component dislocation loops and iron sites has already been shown [22-23]. Until now there was no exact mechanism to explain <c> component loop growth and creation phenomena; however, recently research has shown that <c> loop creation depends on iron sites.

Griffiths [24-25] reviewed microstructure evolution in zirconium and its alloys and also compiled <c> type dislocation characteristics and effective parameters. Griffiths has also analyzed neutron irradiation damage in zirconium and zircaloy-2 and -4 in EBR-II (Experimental Breeder Reactor II) at a temperature range between 644 and 710 K and a fast neutron fluence of 6×10^{22} n/m^2 [26]. The <c> component loops are observed to be much larger in size than the <a> loops, but their density is much lower. Fig. 2 shows typical microstructure characteristic of <c> component dislocation loops.
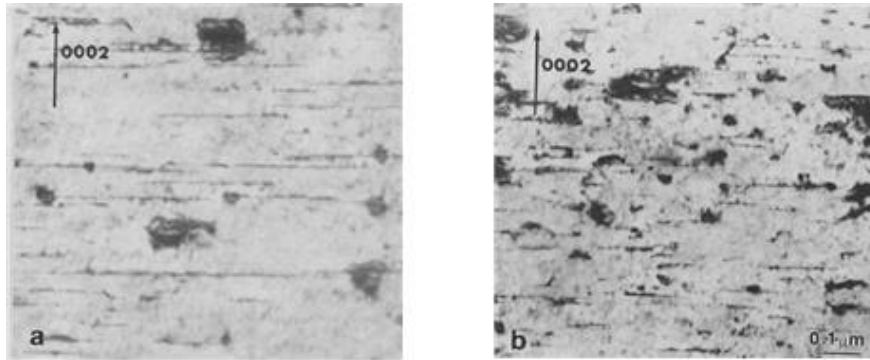
Fig II.12 Irradiation growth strain at 353 and 553 K in annealed and 25% cold-worked zircaloy-2 [28]

2.4 Radiation-induced growth mechanism

In the HCP structure such as zirconium metal, the point-defect diffusion is usually considered to be anisotropic although there is little experimental evidence of this phenomenon. However, from the computer simulation results, it is confirmed that vacancy migration is only slightly anisotropic, but the SIA migration is believed to be significantly anisotropic that is SIA have a higher mobility in the basal plane than along the <c> axis. This DAD has a strong impact on capture efficiency of point defects by sinks.

The fundamental mechanism of irradiation growth is atom rearrangement by defect flux behavior. Historically, quantitative irradiation growth modeling by defect flux behavior was established at 1979 by Holt [29-31] Most recently, Woo expanded Holt work by establishing defect flux mechanism on zircaloy [2]. However until now, sink (grain boundary, dislocation loop, dislocation line, precipitate, defect cluster) effect on zircaloy is not unclear because of fundamental parameter effect is not clear. The theoretical modeling have to be done from atomic level to macrostructure level.

Therefore, this chapter intends is the reveal of the defect flux behavior at zirconium alloy in research reactor by using parameters which was revealed so far. Fortunately defect flux mechanism of single crystal and cold worked polycrystalline were briefly revealed by many researchers [32-34]. Prior to modeling defect flux in research reactor condition, these model need to be reviewed. After that, defect flux to sink will be researched at low temperature.

2.4.1 Single crystal zirconium

In case of single crystal, major sink is only dislocation and dislocation loop. Therefore, irradiation growth begins from developing of dislocation and dislocation loop. Before breakaway region, SIA loop in prism plane is main reason of <a> -axis elongation. However after breakaway region, vacancy loop on basal plane is also main reason of <c> -axis construction.

At first stage of irradiation growth, dislocation and dislocation loop are bias sink because SIA diffusion coefficient is much higher than vacancy diffusion coefficient i.e. $D_i C_i \gg D_v C_v$ (where $D_i \gg D_v$). Therefore SIA loop generated and growth.

At middle stage, dislocation and dislocation loop became neutral sink because vacancy concentration is rapidly increasing. While SIA, which have to recombination with vacancy, disappear at matrix i.e. $D_i C_i = D_v C_v$ (where $C_v \gg C_i$). Therefore growth strain will be saturation.

At last stage, <c> dislocation loop is formed on the basal plane. Therefore, dislocation loop and dislocation on prism plane once again absorb SIA. While SIA concentration is increasing by vacancy loop. Therefore, irradiation growth increases proportionately with radiation dose.
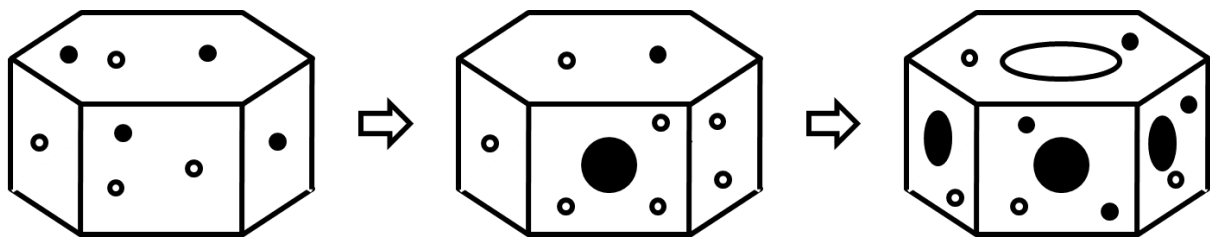
Fig II.13 Defect flux of single crystal zirconium schematic [34]

2.4.2 Annealed polycrystalline zirconium

Annealed zircaloy have low dislocation density cause grain boundary play major role of sink. Therefore, irradiation growth behavior is controlled by defect flux to grain boundary before dislocation loop generated.

At first stage, grain boundaries perpendicular to the basal plane are preferential sinks for SIAs. In contrast, grain boundaries parallel to the basal plane constitute preferential sinks for vacancies. Therefore, first growth occurs by grain boundary

At middle stage, dislocation loops are generated but SIA is already absorbed by grain boundary. It will make dislocation loop become neutrally sink. Also, growth shows saturation tendency.

At last stage, same tendency of single crystal case, vacancy loops are generated and growth behavior shows linear increasing with radiation dose.
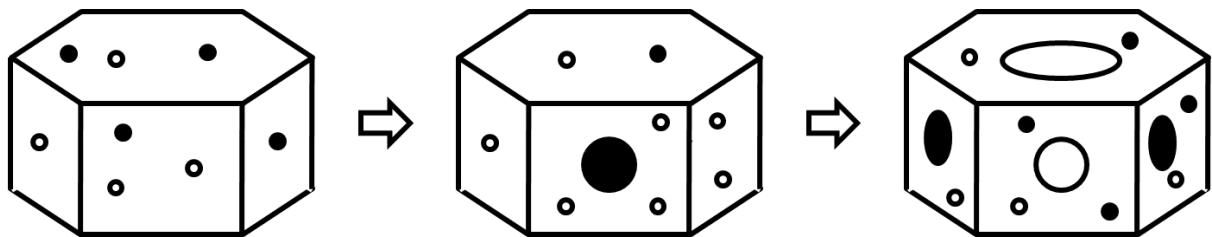
Fig II.14 Defect flux of annealed polycrystalline zircaloy schematic [34]

2.4.3 Cold worked polycrystalline zirconium

In case of cold worked zircaloy, dislocation density is sufficiently high. Therefore dislocation as sink is dominant effect of defect flux on matrix. Growth strain increases linearly in proportion to the radiation dose.
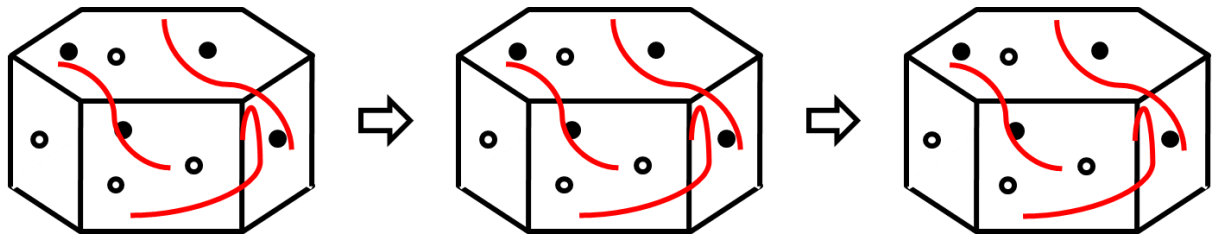
Fig II.15 Defect flux cold worked polycrystalline zircaloy schematic [34]

2.5 Defect rate equation

All of radiation induced phenomenon (creep, segregation, growth and swelling) could be analyzed by two classified parts by time scale. Therefore, quantitative analysis could be done by understanding these two parts. The first part is primary radiation damage which phenomenon occurs below than 10^{-11} sec [35]. In this time scale, radiation induced cascade is created and recovered. The second part is defect flux behavior which phenomenon occurs after 10^{-11} sec. in this time scale, survived defect moving to sink or clustering themselves by thermal diffusion of SIA and vacancy occur. Because this defect flux to sink or clusters is origin of radiation induced dimensional change. Theoretical analysis of should be done in these two parts for quantitative analysis. Therefore, to quantitative analysis of these two parts, each parts are studied by many researcher[35, 36].

Irradiation effect on materials could be analyze by three fundamental parameters (fluence, temperature and materials variable). Because these three parameters consists all of radiation induced phenomena. Among these three parameters, fluence is most important parameter in radiation induced phenomena as the origin all of radiation induced phenomena. Conceptually fluece is basis of the primary radiation damage. Therefore primary radiation damage must be quantified by neutron fluence quantification which is classified energy spectrum to quantitative analysis of irradiation growth.

Dpa is the most basic parameter which could quantitate fluence effect on the materials. Therefore, primary radiation damage can be quantitated by dpa. However, mechanism of the neutron and matrix is complex to analyze. There are for main mechanism (elastic, inelastic, (n, γ), (n, α)). Recently, most researcher use the "specter code" which is published by NRC.

After primary radiation damage quantification, to analyze defect flux, which is occurred by primary raidation damage, in the matrix, material properties and temperature should be analyzed. In case of zirconium, to analyze material properties effect on growth, irradiation growth behavior was compared systemically by single crystal, polycrystalline, and zircaloy. And then growth compared with different temperature range to confirm temperature effect on growth.

The origin of irradiation induced phenomena is the defect flux to sink which means radiation induced mobile defect interaction with sink in matrix. In reactor core, radiation make mobile defect concentration increasing, and microstructure changed. At lastly dimension of materials are changed

Radiation induced dimensional change is occurred by defect flux and defect flux is occurred by defect concentration increasing. Therefore, to quantification of defect flux, defect concentration is needed to be calculated.

The radiation damage theory often call by defect rate equation is rate expression of defect concentration and sink concentration, Therefore, Defect rate equation is one of the important method to get defect flux behavior mathematically. Defect rate equation is the mathematical expression of radiation induced defect quantity and quality. Hence quantification of radiation induced defect concentration is the essential part of theoretical radiation induced deformation modeling.

Because defect rate equation is the basic part of radiation induced phenomena, it is researched from uranium to structure materials. The early stage defect rate equation, the basic assumption about the radiation-induced defect was considered only one type that point defect (frenkel pair) [1, 2]. However, in that framework, theoretical modeling of radiation effects on metal was not well fit experimental result [37].

These problems were solved by adopting the concept of radiation damage morphologies [38]. In the 1990s, Woo and Singh modified the incorrect framework by adopting the cascade concept that radiation damage produced not only point defects but also clusters [3, 4].

2.5.1 Primary radiation damage

The radiation-induced defect generation sequence could be classified by two parts. The first part is primary radiation damage which is composed with cascade generation and relaxation phenomena. In these phenomena, atom behavior was explained by kinetics and atomic fluctuation. This phenomena occurs so quickly ($< 10^{-11}$). Therefore, in this time region, atom diffusion dose not considering.

Irradiation effect on materials, composed four main mechanism (elastic, inelastic, (n, γ), (n, α)). These mechanism also could be classified by two parts, one is the neutron and matrix interaction, which mean PKA (primary knock on atom) are generated. The second is the PKA and matrix interaction. In this interaction secondary knock on atom, ternary knock on atom are generated.

To measure the secondary phenomena, PKA effect on the matrix, many model are proposed. In 1972, NRT model was proposed and until now NRT model are using as international standard

$$\nu(T) = \frac{k(E - S_e)}{2E_d}(NRT) \tag{II.1}$$

Where E is the total energy of the PKA, S_e is the energy lost in the cascade by electron excitation, E_d is damage energy.

Above equation could calculate PKA effect on matrix. However to calculate over all neutron effect we have to calculate average cross section of the neutron spectrum. Below equation could calculate average neutron cross section

$$\sigma_D(E_i) = \int_{\check{T}}^{\hat{T}} \sigma_D(E_i, T) \nu(T) \mathrm{dT} = \int_{\check{\phi}}^{\hat{\phi}} \sigma_D(E_i, \phi) \nu(T) \mathrm{d\Omega} \tag{II.2}$$

$\sigma_D(E_i, T)$ the probability that a particle of energy E_i impart a recoil energy T to a struck lattice atom, $\nu(T)$ = the number of displaced atoms. After calculate the average cross section of the various neutron spectrum, it could calculate the number of the defect which is induced neutron.

$$R_d = N \int_{\check{E}}^{\hat{E}} \phi(E_i)\sigma_D(E_i)dE_i \qquad \text{(II.3)}$$

$$G_{NRT} = N \int_{E}^{\hat{E}} \Phi(E_i)\sigma_D\left(E_i\right)dE_i \qquad \text{(II.4)}$$

Where N is the lattice atom density, $\Phi(E_i)$ is the energy-dependent particle flux, $\sigma_D(E_i)$ is the energy-dependent displacement cross section. This equation could be simplified after some mathematical calculation. In these days, SPECTER code [39], which use this equation, is most widely used by many researcher.

2.5.2 Simple balance equation

The simplest defect rate equation was made by Sizmann, from this balance equation model, it could be calculated that defect concentration in matrix which could be expressed by three terms. K_o is defect production rate. It could be calculated from G_{NRT} term by considering cascade relaxation. K_{iv} is recombination rate which mean vacancy and SIA are combine and go to perfect lattice atom, the last term K_{vs} & K_{is} means that total sink strengths of all the extended defects in the material. C_i and C_v a is defect concentration of SIA and vacancy. And C_s^T is total sink strength of matrix.

$$\frac{dC_v}{dt} = K_o - K_{iv} C_i C_v - K_{vs} C_v C_s^T \tag{II.5}$$

$$\frac{dC_i}{dt} = K_o - K_{iv} C_i C_v - K_{is} C_i C_s^T \tag{II.6}$$

Defect rate equation is the mathematical expression of radiation induced defect quantity and quality. Hence quantification of radiation induced defect concentration is the essential part of theoretical irradiation growth modeling. Therefore, defect rate equation is must needed to irradiation growth modeling. It is researched from uranium to structure materials.

This early stage defect rate equation, assumed that radiation-induced defect is composed only one type that point defect (frenkel pair) [1, 2]. However, in that framework, theoretical modeling of radiation effects on metal was not well fit experimental result. These problems were solved by adopting the concept of radiation damage morphologies. In the 1990s, Woo and Singh modified the incorrect framework by adopting the cascade concept that radiation damage produced not only point defects but also clusters [3, 4].

After cascade generation and relaxation time region, defect are composed two type that point defect and cluster defect. These phenomena also could be mathematically expressed by balance equation from defect generation term. But we also should consider cluster rate equation. From this improved balance equation, it could know that defect concentration at any given time.

2.6 Radiation-induced growth strain equation

As referred before, irradiation growth is occurred by defect flux. Therefore, growth stain could be calculated after defect rate equation are established. Although irradiation growth express differently by several author, all equation have same physical meaning that defect accumulation of sink. This physical mechanism are generally expressed by dislocation climb mechanism. The general formula of climb mechanism could be describe by simple equation.

$$\frac{d\varepsilon_{\mathrm{a,c}}}{dt} = \rho b V \tag{II.7}$$

$$V = \frac{1}{b}\left(Z_i D_i C_i - Z_v D_v C_v\right) \tag{II.8}$$

where ρ is dislocation line and dislocation loop density, b is bugers vactor, V is dislocation climb velocity, D_i and D_v is diffusion coefficient of interstitial and vacancy, C_i and C_v are SIA and vacancy defect concentration and Z_i and Z_v are SIA and vacancy bias factor. From these equation, irradiation growth could be calculated by specific sink type. The bias factor is also referred capture efficient factor because this factor physically determine that how many defect are absorbed to the sink density. Therefore defect flux meaning is number of defect which is absorbed unit sink density. In case of hexagonal close pack system, bias factor is changed by DAD, hence crystal structure has anisotropy property [8].

Among the many equations, Holt and Golubov's growth equation is best option that most well explains irradiation growth phenomena. In Holt equation, irradiation growth are calculated in time independent.

$$\varepsilon_d = \left(N_{iy} - Nvy\right)\Omega Ady = \left(Niy - Nvy\right)\Omega \sum_{\omega} Xy(\omega)cos2\omega \tag{II.9}$$

Here, Niy, Nvy is defect number which is accumulated dy sink. The sink direction is and atom volume is Ω. However, in case of S.I Golubov equation. Irradiation growth are expressed by time dependent because of defect number density could be replaced by dislocation climb velocity.

$$\frac{d\varepsilon_{\mathbf{a}}}{dt} = \sum_m \rho_m V_m b_m \cos^2 \varphi_m = \sum_m \rho_m \left(D_i C_i - D_v C_v \right) \cos^2 \varphi_m \qquad \text{(II.10)}$$

Here, ρ_m is dislocation sink density, V_m is dislocation climb velocity, b_m is burgers vector, and $\cos^2 \varphi_m$ is angel between c axis and sink direction.

2.7 Radiation-induced growth models

Experiment of irradiation growth have been done many researchers after Buckly [9]. From these experiments, qualitatively mechanisms are suggested by using microstructure analysis and then, defect rate theory is used to calculation of defect concentration for quantitatively modeling. Historically, Hesketh [40] and Carpenter [41] set up firstly theoretical growth modeling by experiment database. After that, theoretical modeling base on rad theory developed by Dollins [42], Fainsteins - Dedraz [43], MacEWEN [44] and Bullough [45] who adopt rate theory in earnest.

However, these papers, published in 1980s, had limitation that it is assumed that defect are composed only point defect and point defect diffusion isotropy. Therefore, quantitative equation was not fully contain microstructure information. Therefore, the mechanism is not agree with real irradiation phenomena

In the after of 1980s, noticeable theoretical modeling paper is about sink strength in zirconium was published by Woo [8]. He considered difference of the SIA diffusion coefficient <a> axis and <c> axis. Therefore bias factor could be developed at each sink in the zirconium matrix. Until now this modeling give fundamental base in the growth research area.

Recently, microstructure analysis and computer simulation was developed and also theoretical analysis by computer code was advanced. From these evolutions, irradiation growth modeling is researched again to fundamental understanding. Christien [32] had been theoretical modeling with frenkel pair three diffusion model (FP3DM)in single crystal. And after that Golubov [33] also modeling in single crystal with production bias modeling (PBM) modeling. FP3DM physically means mobile defect compose only point defect and PBM means defect are generated both of point defect and cluster defect and also assume SIA could mobile 1D.

More specifically, in Christien work, he assumed that main sink is dislocation loop and line. <a> elongation occurs by <a> dislocation loop growth. <c> shortening occurs by vacancy relaxation. This equation shows <a> & <c> axis elongation and shortening by Chistien's method. From he's equation, irradiation growth result show good agreement of experimental data. In case of Golubov, as like Christien, he assumed that main sink is dislocation loop and line, and elongation occurred by dislocation loop climb. However, using specific technic, defect rate equation does not needed for irradiation growth calculation.

2.7.1 Carpenter's model (1975)

Before the development of irradiation growth model, which is based on the rate theory, the experimental growth prediction modeling was established by using loop growth. From simple three assumption that loops all have the same SIA character, specimen has 100% texture and loop has same bugers vector, he calculates maximum irradiation growth by loop growth concept.

At that time, by measuring of the defect size and concentration, it could know that existent of point defect in matrix effect on the irradiation growth is negligible. Therefore, an alternative mechanism is suggested, based on the bias interaction between SIAs and dislocations.

Assumption of Irradiation Growth:

Dislocation loop have to be defined its characteristic In order to calculate irradiation growth. It was difficult to measure small sizes of the loops. He use extreme upper-bound values of strain assumption.

(1) All loops have the same character (SIA) and same burgers vector

(2) The specimen has 100% texture so that it behaves like a single crystal

(3) Growth occurred by dislocation climb mechanism
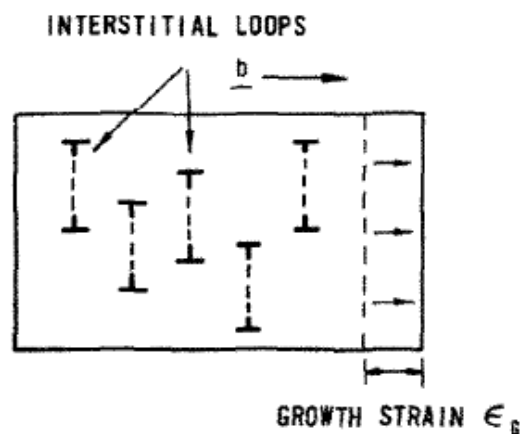
Fig II.16 Schematic of assumption of Carpenter model

Result of the Carpenter's model:

In practice, at least half the upper bound value assuming there is equal probability of occurrence of the three type Burgers vectors. In Fig II.17, experimental growth measurements for annealed and cold-worked Zircaloy-4 [46, 47] and the calculated results are plotted . It is clear that the calculated strain from the microstructure analysis is far less than the experiment data, at large fluences, calculation irradiation growth data was saturated.
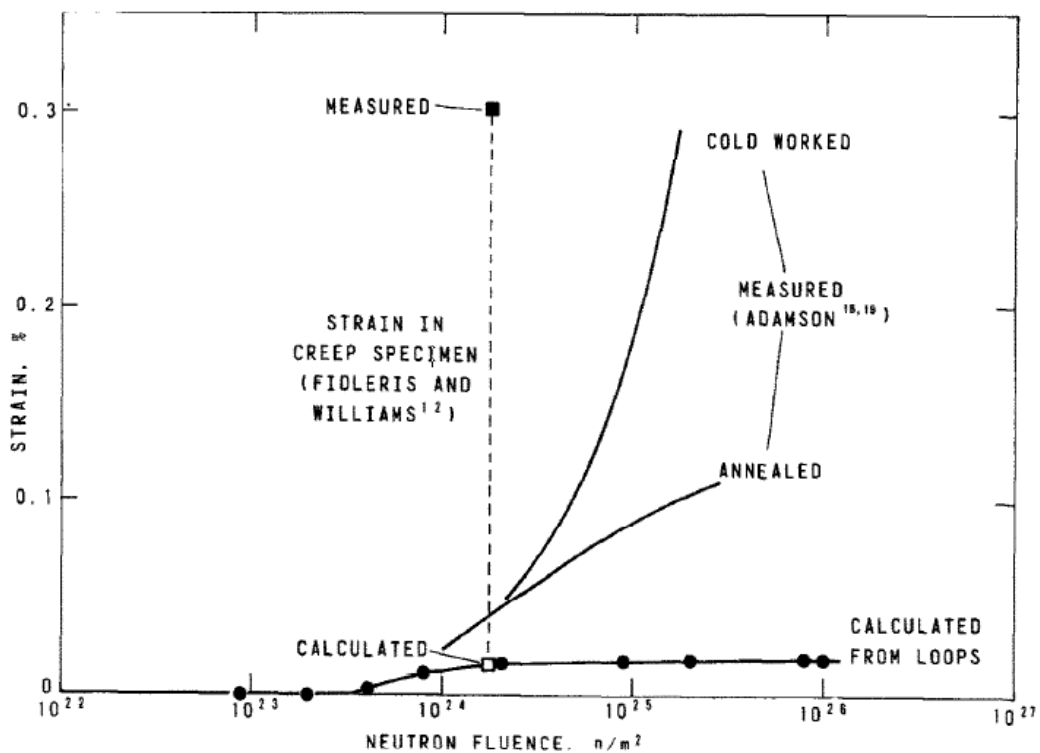
Fig II.17 Growth modeling result of Carpenter

2.7.2 Dollins's model (1978)

Dollins firstly adopt defect rate equation for the calculation of the irradiation growth. From the buckley frame work, he assume that only four major sink such as dislocation line, loop, grain boundary and depleted zone.

In defect rate equation, vacancies and interstitials are annihilate through recombination or through loss to dislocations, dislocation loops, depleted zones, or grain boundaries. The specific sink defect rate equation could be expressed by defect rate equation.

Assumption of Irradiation Growth:

Network dislocation (loop & line) and grin boundary characteristic are considered as major sink in the matrix. In case of polycrystalline, texture is most important parameter in modeling. Texture effect are considered by f-factor

(1) All loops have the same character (SIA) and same burgers vector

(2) Growth occurred by dislocation climb mechanism

(3) Dislocation line, loop, grain boundary and depleted zone and grin boundary are major sink

(4) Texture effect are considered by f-factor

(5) Interstitial type sink is dislocation loop and line

(6) Dislocation is anisotropically distributed before the irradiation

(7) Vacancy type sink is grain boundary & depleted zones

(8) Sink strength of vacancy and interstitial are different

Result of the Dollins's model:

Fig II.18 shows theoretical predictions of growth strain for cold worked Zircaloy. Calculation result indicates that growth strain increases with degree of cold work or the dislocation density. The experimental data is based on Hesketh [48] data for cold worked Zircaloy-2 with an f-factor number of 0.05. Unfortunately, in dollins paper, specific explain about the gab of theoretical result and experiment result does not provide.
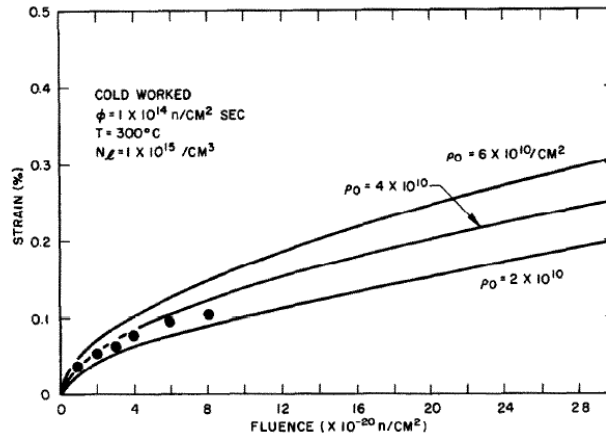
Fig II.18 Growth modeling result of Dollins

In case of annealed polycrystalline, growth strain versus fluence material is shown in Fig II.19. The growth dependence of changing of the interstitial dislocation loop density is also shown.
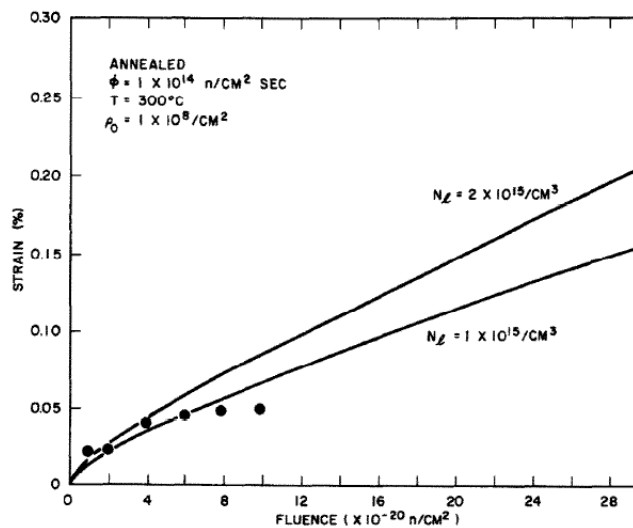
Fig II.19 Growth modeling result of Dollins

2.7.3 FSP's model (1978)

As like Dollins, Fainstein-Pedraza, E.J. Sawno and A.J. Pedraza (FSP) using same technic that net defect flux and dislocation characteristic was used to analyze of irradiation growth. However, in FSP modeling, he using only two major sink (network dislocation and grain boundary) and this two major sink are well reflect manufacture process effect on growth.

This modeling was well fit the experiment of annealed zirconium. However in cold worked zirconium is not well matched. He also calculated loop size and density for verification of the calculated growth. From this equation, also, annealed zirconium was well agree with polycrystalline as like growth strain results however, it was also failure to explain the loop growth of cold worked is not well fit.

Assumption of Irradiation Growth:

Network dislocation (loop & line) and grin boundary characteristic are considered as major sink in the matrix. In case of polycrystalline, texture is most important parameter in modeling.

(1) All loops have the same character (SIA) and same burgers vector

(2) Growth occurred by dislocation climb mechanism

(3) Network dislocation (loop & line) and grin boundary are major sink

(4) Texture effect are considered by f-factor

(5) Interstitial type sink is dislocation loop

(6) Dislocation is anisotropically distributed before the irradiation

(7) Vacancy type sink is grain boundary & depleted zones

(8) Sink strength of vacancy and SIA are different

Result of the FSP's model:

In Fig II.20, Adamson's experiment results are reported by Fidleris [14]. Fitting the data corresponding to each amount of cold-work induced dislocation density. Kreyns's data [49] also show same tendency of Adams results.

If the neutron flux is known, growth strain could be calculated. The theoretical result could be seen that fairly good agreement with the experimental ones.
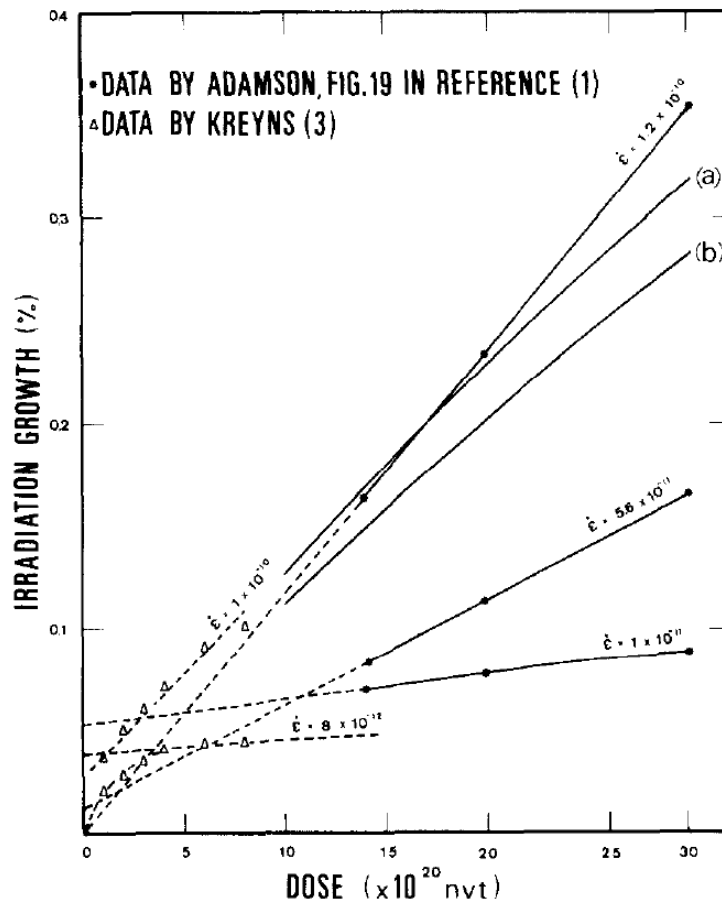
In Fig II.20 Growth modeling result of FPS

2.7.4 Christen's model (2008)

Recently, microstructure analysis and computer simulation was developed and also theoretical analysis by computer code was advanced. From these evolutions of research area, irradiation growth is researched again to consider these advanced things. Christien had been theoretical modeling with frenkel pair three diffusion model in single crystal Chisten's work has limitation that he assume vacancy do not react with sink and it's application region is limited to single crystal.

Assumption of Irradiation Growth:

Vacancy are do not react any sink until $<c>$ loop is appeared, so he assume that vacancy concentration in materials will be preserved as it generated except recombination. However in case of interstitial diffusion coefficient so faster than vacancy assumed that loop flux, dislocation flux, surfaces flux and preserved in matrix. Radiation-induced defect could expressed by loop growth in prims plane because defect flux to sink in only dislocation line and dislocation loop single crystal.

(1) All loops have the same character (SIA) and same burgers vector

(2) Growth occurred by dislocation climb mechanism

(3) Network dislocation (loop & line) are major sink

(4) Interstitial type sink is $<a>$ type dislocation loop

(5) Vacancy type sink is $<a>$ type dislocation loop

(6) Sink strength of vacancy and SIA are different cause by DAD

(7) Interstitial react only network dislocation(loop & line)

(8) Iron precipitation play the seed of $<c>$ dislocation loop

(9) Cluster defect was neglected

Result of the Christien's model:

Fig II.21 shows that the calculated growth strain, which fit the experimental points very well by using <c> type loops. It is noticeable that the general shape of the growth curves and particularly the occurrence of breakaway growth is very satisfactorily modelled. All of the three stage, experiment results [13] was well matched. However, unfortunately, precipitation effect on growth was not well explained by theoretically. Moreover, diffusion coefficient was now well matched computer simulation results.
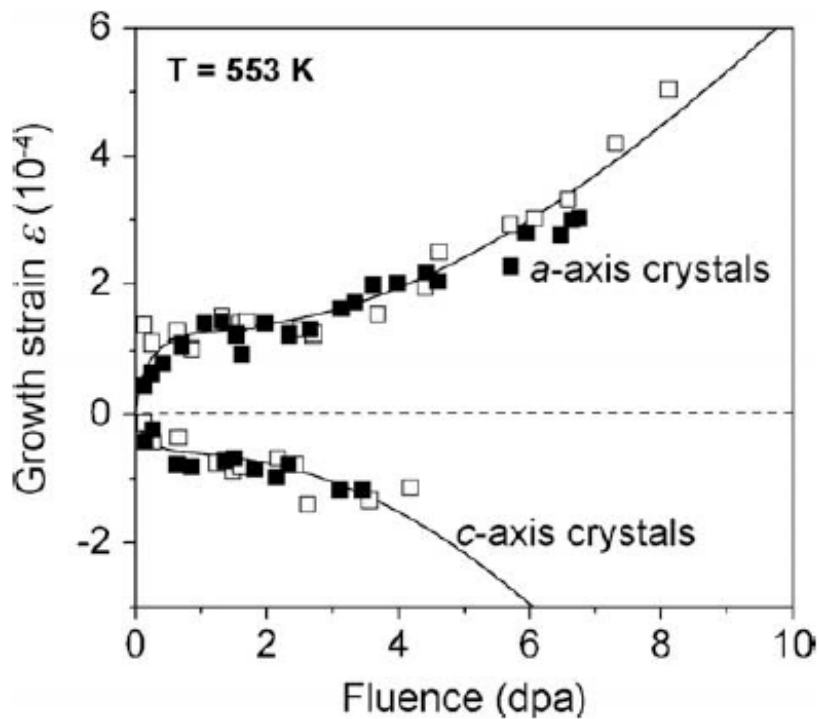
Fig II.21 Growth modeling result of FPS

2.7.5 Golubov's model (2008)

In case of Golubov works, the majority of framework are exactly same of Christien method. Like as Christien, he assumed that growth occurs when defect climb dislocation and dislocation loop. The result show good agreement of experiment irradiation growth and also Golubov have same limitation of Christien, that application reason is limited to single crystal. However, unlikely Christien, he assume that cluster defect also created and using assumption ,which is defect concentration is steady state, growth are calculated without defect rate equation. From these assumption, irradiation growth are calculated.

Assumption of Irradiation Growth:

For the simple calculation, he neglect the recombination term. However, he consider cluster defect. In case of cluster defect, sink strength are calculated by same method of dislocation loop. Eventually defect irradiation growth are calculate by two source that point defect and cluster defect accumulation at dislocation loop.

(1) All loops have the same character (SIA) and same burgers vector

(2) Growth occurred by dislocation climb mechanism

(3) Network dislocation (loop & line) are major sink

(4) Interstitial type sink is <a> type dislocation loop

(5) Vacancy type sink is <a> type dislocation loop

(6) Sink strength of vacancy and SIA are different cause by DAD

(7) Interstitial react only network dislocation(loop & line)

(8) Iron precipitation effect was neglected

(9) Cluster defect was considered

Result that of the Golubov's model:

Fig II.22 shows that the calculated growth strain of Goluobv, as like Christien case, growth result are well matched experimental results [13]. Unfortunately, theoretical analysis of dislocation loop was not fully developed, breakaway region is hard to predict. Therefore, experiment number density of dislocation loop are suggested. From this experimental results, growth was calculated and results are well matched. However, in case of this model is also diffusion coefficient information was unclear. Therefore, more fundamental computer simulation should be done in this part.

Fig II.22 Growth modeling result of Golubov

III. Rationale and Approach

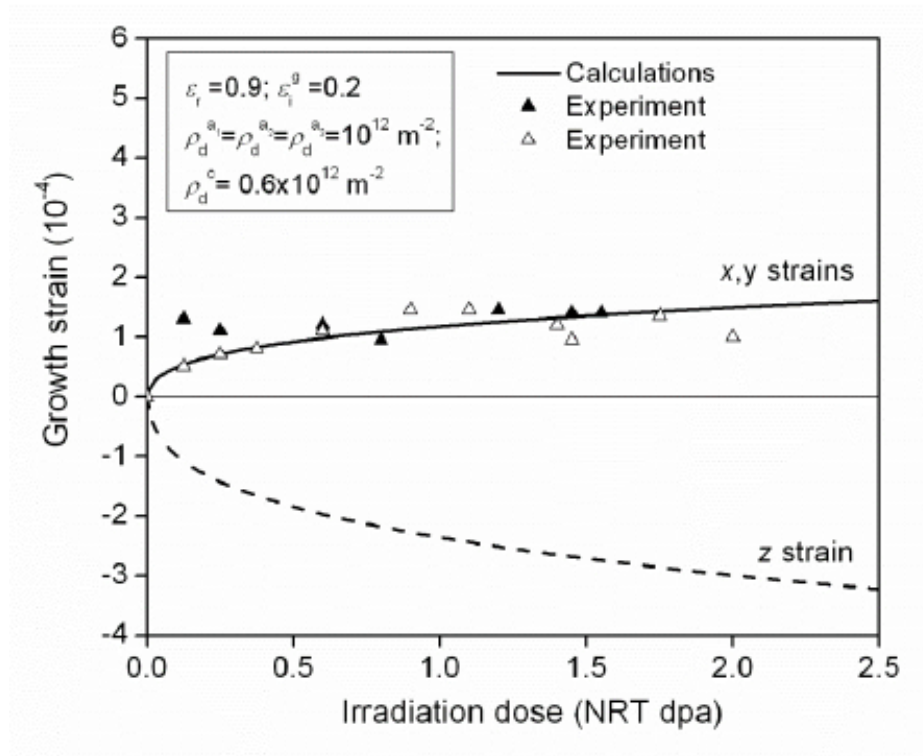At the literature study chapter, irradiation growth research trend is reviewed. At the early stage of the growth research field, defect rate theory and microstructure information are developed and from this efforts, it was possible to make irradiation growth modeling. After that, more specific experiment data and improved theoretical modeling are developed. In these days single crystal has been review two author. However, in case of polycrystalline, dislocation loop is not main sink to contribute irradiation growth. GB is the main sink of the irradiation growth. Therefore it is difficult to calculate GB sink strength and anisotropy factor by using "f" factor. Until now there is not general model to predict polycrystalline growth modeling. Therefore, in this paper single crystal modeling will be extended to polycrystalline modeling by using assumption which is used single crystal (DAD, loop increasing modeling)

Dislocation Loop Modeling

Firstly, python code is used to modeling for single crystal irradiation growth. Before the 3dpa, it has been assumed <c> dislocation loop is not existed, therefore irradiation growth will be saturated. The saturation of the irradiation growth strain is mimicked. After 3 dpa, <c> dislocation loop was appeared, therefore growth strain was increasing because defect flux behavior was different. This phenomenon also reflected to python cod modeling.

Grain Boundary Modeling

In case of polycrystalline, dislocation loop are has been analyzed that both of vacancy and SIAloop are existed. Therefore loop is not major sink to effect irradiation growth. Especially, irradiation growth at 553K dislocation proportion between vacancy and SIAloop density analyze that 50 % : 50 %. Therefore in the polycrystalline modeling GB was assumed that main parameter to effect of polycrystalline.

Dislocation Line Modeling

At lastly, cold work zircaloy was modeled by using assumption that initial dislocation density is main sink. In case of cold worked zircaloy, dislocation density is much larger than any other sink density therefore, sink strength of initial dislocation line is main parameter of the cold worked zircaloy.

Lastly, this fundamental defect behavior will be compare with material microstructure. Because material microstructure is fundamental to macro-scale behavior, understanding the correlation between

microstructure and theoretical model may explain radiation-induced growth. In the case of zirconium and its alloys, microstructure changes dramatically with radiation-induced defects, which can be clustered into two major dislocations. Thus, dislocation can be used conceptually to analyze irradiation growth in zirconium and its alloys.
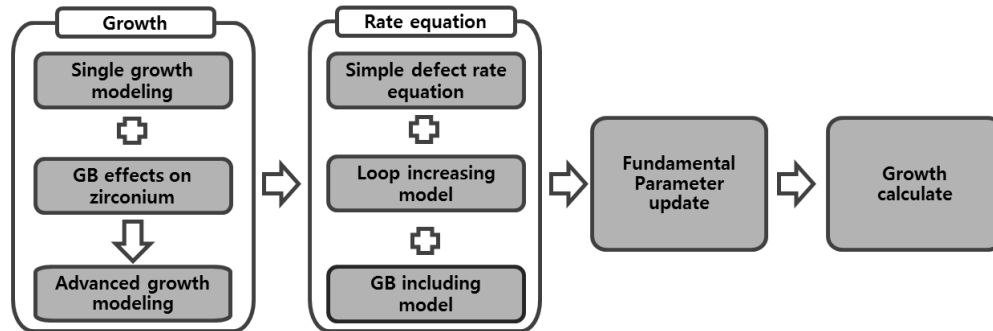
Fig III.1 Procedure of research progress

IV. Results

From the improved defect rete theory, improved irradiation growth model are made and growth results are calculated from single to zircaloy. Firstly, Irradiation growth modeling is conducted in commercial reactor condition because there is more extensive research data than commercial reactor. In this chapter, growth modeling specifically and results are presented.

4.1 Improved defect rate equation

Before to explain in detail about defect rate equation, it should be understood that defect flux concept. As referred microstructure analysis chapter, the origin of the irradiation growth is atom rearrangement by cascade damage. Therefore, the physical meaning of defect flux is defect accumulation at sink hence defect flux equation is composed of multiply of diffusion coefficient and defect concentration parameter. From this equation, it could be calculated that number of defect which accumulated at sink per unit time. Diffusion coefficient could be calculated more easily than defect concentration parameter by experiment and computer simulation. However, in case of defect concentration, it is difficult to analyze by experiment. Therefore, so far, historically, defect concentration is calculated by balance equation. In this papers, defect rate equation are established from single to poly. And each sink strength are followed recent method that dislocation loop sink strength was time dependent and dislocation line and grain boundary is constant. The dislocation loop sink strength equation follow Golubov paper [33]. Also because of DAD effect on the sink strength, each sink are separated by two term by axis direction. One is parallel with <c> direction and second is parallel with <a> direction. The detail input parameter are given in table 1.

Table 1.Input parameters

Input parameter		Symbol	Unit	value
Defect generation rate		G	dpa s^{-1}	10^{-7}
Recombination radius		r_{iv}	cm	10^{-7}
Burgers vector		b	cm^{-2}	3.23×10^{-8}
Diffusion coefficient	Vacancy	D_v	cm^2 s^{-1}	3.0×10^{-17}
	SIA	$\overline{D}_i$	cm^2 s^{-1}	1.0×10^{-6}
Sink strength	<a> SIA loop	ρ_{ilp}	cm^{-2}	$2\pi r_i N_i$
	<a> V loop	ρ_{vlp}	cm^{-2}	$2\pi r_v N_v$
	<c> V loop	ρ_{vlb}	cm^{-2}	$2\pi r_v N_v$
	<a> dislocation line	ρ_{dp}	cm^{-2}	Single:7.25x10^6 Cold:20x10^9
	<c> dislocation line	ρ_{db}	cm^{-2}	Single:2.25x10^6 Cold:5x10^9
	<a> GB	$(k_{GB}/2)$	cm^{-2}	$6 \times \sqrt{\rho} \div d_{gb}$
	<c> GB	$(k_{GB}/2)$	cm^{-2}	$6 \times \sqrt{\rho} \div d_{gb}$
Average strain factor	<a> SIA loop	A_{ilp}	Constant	0.5
	<a> V loop	A_{vlp}	Constant	0.5
	<c> V loop	A_{vlb}	Constant	1.0
	<a> dislocation line	A_{dp}	Constant	0.5
	<c> dislocation line	A_{db}	Constant	1.0
	<a> GB	A_{GBp}	Constant	0.5
	<c> GB	A_{GBp}	constant	0.5
Bias factor	<a> SIA loop	Z_{ilp}^i	Constant	1.56
	<a> V loop	Z_{vlp}^i	Constant	0.586
	<c> V loop	Z_{vlb}^i	Constant	0.586
	<a> dislocation line	Z_{dp}^i	Constant	1.56
	<c> dislocation line	Z_{db}^i	Constant	0.586
	<a> GB	Z_{gp}^i	Constant	0.156
	<c> GB	Z_{gb}^v	Constant	0.586

4.1.1 Single crystal zirconium

For calculation of the growth strain, it has to calculated defect concentration, In case of single crystal zirconium, dislocation loop and dislocation line are the main sink in the matrix. Therefore, the defect rate equations could be simply composed that defect generation, recombination and loss of sink such as dislocation loop and line. In case of loss of sink, each sink are separated by sink direction because of DAD effect. Although same type of sink, defect strength is different by sink direction.

$$\frac{dC_{sv}}{dt} = K_o - K_{iv}C_iC_v - \rho_{ilp}Z_{ilp}^v C_v D_v - \rho_{vlb}Z_{vlb}^v C_v D_v - \rho_{dp}Z_{dp}^v C_v D_v - \rho_{db}Z_{db}^v C_v D_v \qquad \text{(IV.1)}$$

$$\frac{dC_{si}}{dt} = K_o - K_{iv}C_iC_v - \rho_{ilp}Z_{ilp}^i C_i D_i - \rho_{vlb}Z_{vlb}^v C_i D_i - \rho_{dp}Z_{dp}^i C_i D_i - \rho_{db}Z_{db}^i C_i D_i \qquad \text{(IV.2)}$$

$$\rho = \rho_{dp} + \rho_{db} + 2\pi r_v N_v + 2\pi r_i N_i \qquad \text{(IV.3)}$$

Where K_o is defect production rate. K_{iv} is recombination rate which mean vacancy and SIA are combine and go to perfect lattice atom. ρ_{ilp}, ρ_{dp}, ρ_{vlb}, ρ_{db} are each sink density. Z_{ilp}^i and Z_{ilp}^v are SIA and vacancy bias factor of SIA loop, Z_{dp}^i and Z_{dp}^v are SIA and vacancy bias factor of dislocation line, Z_{vlb}^i and Z_{vlb}^v are SIA and vacancy bias factor of vacancy loop, Z_{db}^i and Z_{db}^v are SIA and vacancy bias factor of dislocation line. C_{si} and C_{sv} are defect concentration of SIA and vacancy in single crystal matrix, D_i and D_v are diffusion coefficient in the matrix.

The equation (IV. 3) is about to total dislocation loop and line density. Although dislocation line assume to be constant, dislocation loop is assumed time dependent parameter. The r_v and r_i are dislocation loop radius of vacancy and interstitial and N_v and N_i are dislocation loop number density of vacancy and SIA. In case of loop number density, it is hard to calculate by theoretical method because there is

45

not general loop nucleation and growth equation in radiation situation. Therefore experiment value of loop number density was used. However, in case of dislocation loop radius, could be calculated by theoretical equation.

$$r_v = \sqrt{(S_v / \pi b N_v)} \qquad \text{(IV.4)}$$

Where S_v is total number of the vacancy dislocation loop. Also change of the total number of dislocation loop is proportion with probability of defect interaction. Therefore, total number defect in loop could be calculated with defect rate equation.

$$\dot{S}_v = 2\pi r_v N_v (D_v C_v - D_i C_i) \qquad \text{(IV.5)}$$

In case of SIA dislocation loop, radius and number density could be calculated by Form this equation. Although equation are established, all of physical phenomenon could not be simulated because theoretical and code structure development. In this modeling case, it should be consider that dislocation loop generation and saturation behaviors. This dislocation behavior are simulated by dislocation loop number density function.

4.1.2 Polycrystalline zirconium

In case of polycrystalline zirconium, basically dislocation loop and line should be considered as main sink in the matrix and also GB have to be added in rate equation. Therefore, the defect rate equations are more complex than single crystal case. However using single crystal defect rate equation, defect rate equation could be simply expressed. In the equation, grain boundary sink strength are calculated by using MacEWEN [44] method.

$$\frac{dC_{pv}}{dt} = \frac{dC_{sv}}{dt} - k_{gp}^2 Z_{gp}^v C_v D_v - k_{gp}^2 Z_{gp}^v C_v D_v \qquad \text{(IV.6)}$$

$$\frac{dC_{pi}}{dt} = \frac{dC_{si}}{dt} - k_{gp}^2 Z_{gp}^i C_i D_i - k_{gb}^2 Z_{gb}^i C_i D_i \qquad \text{(IV.7)}$$

$$k_{gb}^2 = 6 \times \sqrt{\rho} \div d_{gb} \qquad \text{(IV.8)}$$

Where C_{pi} and C_{pv} is defect concentration of SIA and vacancy in polycrystalline matrix. k_{gp}^2 and k_{gb}^2 are grain boundary sink strength. Z_{gp}^i and Z_{gp}^v are SIA and vacancy bias factor of grain boundary in prism. Z_{gb}^i and Z_{gb}^v are SIA and vacancy bias factor of grain boundary in basal plane.

4.2 Improved radiation-induced growth equation

In case of growth strain equation. From qualitative analysis of mechanism, irradiation growth modeling could be developed. So far, several growth equation are already established many authors. Although these equation is expressed differently by many author, eventually these equation could be expressed by reaction probability between defect and sink. Because they have same physical meaning that atom rearrangement by defect flux. In this paper, growth modeling is established same manner that previous modeling developing method. Therefore, in this equation, irradiation growth is calculated with sink strength multiply and defect flux and anisotropy factor. The anisotropy factor is induced each grain boundary orientation. Therefore, in case of single crystal, elongation occur uniform direction. However, in case of polycrystalline, elongations are occurs at any given direction. From anisotropy factor, irradiation growth could be calculated at certain direction. The anisotropy factor of certain direction could be obtain at experiment reference. Moreover, in this modeling, growth strain are calculated by each sink type and crystallographic effect was included by modified bias factor. And modeling developed by two part such as single crystal and polycrystalline.

4.2.1 Single crystal zirconium

In case of single crystal, irradiation growth equation is simple compare with the polycrystalline because a-axis elongation and c-axis shortening could be directly expressed. Therefore irradiation growth equation is

$$\frac{d\varepsilon_a^{ilp}}{dt} = A_{ilp}\rho_{ilp}\left(Z_{ilp}^i D_i C_i - Z_{ilp}^v D_v C_v\right) \tag{IV.9}$$

$$\frac{d\varepsilon_a^{dp}}{dt} = A_{dp}\rho_{dp}\left(Z_{dp}^i D_i C_i - Z_{dp}^v D_v C_v\right) \tag{IV.10}$$

$$\frac{d\varepsilon_c^{vlb}}{dt} = A_{vlb}\rho_{vlb}\left(Z_{vlb}^v D_v C_v - Z_{vlb}^i D_i C_i\right) \tag{IV.11}$$

$$\frac{d\varepsilon_c^{db}}{dt} = A_{db}\rho_{db}\left(Z_{db}^i D_i C_i - Z_{db}^v D_v C_v\right) \tag{IV.12}$$

$$\frac{d\varepsilon_a}{dt} = \frac{d\varepsilon_{ilp}}{dt} + \frac{d\varepsilon_{dp}}{dt} \tag{IV.13}$$

$$\frac{d\varepsilon_c}{dt} = \frac{d\varepsilon_{vlb}}{dt} + \frac{d\varepsilon_{db}}{dt} \tag{IV.14}$$

In this equation, ϵ_a^{ilp}, ϵ_a^{dp}, ϵ_a^{vlb}, ϵ_a^{db} are irradiation growth strain induced by SIA dislocation loop in prism plane, dislocation line parallel with prism plane ,vacancy dislocation loop in basal plane and dislocation line parallel with basal plane, A_{ilp}, A_{dp}, A_{vlb}, A_{db} are strain average factor of each sink, ρ_{ilp}, ρ_{dp}, ρ_{vlb}, ρ_{db} are each sink density. Z_{ilp}^{i} and Z_{ilp}^{v} are SIA and vacancy bias factor of SIA loop, Z_{dp}^{i} and Z_{dp}^{v} are SIA and vacancy bias factor of dislocation line, Z_{vlb}^{i} and Z_{vlb}^{v} are SIA and vacancy bias factor of vacancy loop, Z_{db}^{i} and Z_{db}^{v} are SIA and vacancy bias factor of dislocation line and ϵ_a is total strain of <a> axis irradiation growth. Among these sink density, dislocation loop is dependent variable of defect flux. It will be treat specifically next defect rate equation chapter. And average strain factor is growth strain proportion with <a> axis and <c> axis elongation. In case of <a> dislocation loop and dislocation line average stain factor, which is perpendicular with <c> axis has 0.5 value, whilst <c> dislocation loop and dislocation line, which is perpendicular with <c> axis has 1 value [42].

4.2.2 Polycrystalline zirconium

In case of annealed polycrystalline zirconium, grain boundary sink and orientation (texture) have to be considered in growth equation and these parameters are became most important parameter. Therefore, irradiation growth equation is expressed differently from the single crystal. Texture is that average fraction of the single grains direction at specific axis in Cartesian coordinate system. Therefore, growth modeling results at given direction could be controlled by texture.

For the calculation of the growth modeling at specific given direction of the polycrystalline, firstly single grain growth strain of <a>and <c> axis strain should be calculated, after that, anisotropy factor of polycrystalline is need to be calculated by texture. The growth equation which contain of grain boundary effect is expressed by

$$\frac{d\varepsilon_a^{gp}}{dt} = A_{gp}\rho_{gp}\left(Z_{gp}^i D_i C_i - Z_{gp}^v D_v C_v\right)$$
(IV.15)

$$\frac{d\varepsilon_c^{gb}}{dt} = A_{gb}\rho_{gb}\left(Z_{gb}^i D_i C_i - Z_{gb}^v D_v C_v\right)$$
(IV.16)

$$\frac{d\varepsilon_d}{dt} = A_{poly} \times \left(\frac{d\varepsilon_a^{ilp}}{dt} + \frac{d\varepsilon_a^{dp}}{dt} + \frac{d\varepsilon_a^{gp}}{dt}\right)$$
(IV.17)

In this equations, ϵ_a^{gp} and ϵ_a^{gb} irradiation growth strain induced by grain boundary in prism and basal plane, A_{gp} and A_{gb} are grain boundary in prism and basal plane average strain factor, k_{gp}^2 and k_{gb}^2 are grain boundary sink strength. Z_{gp}^i and Z_{gp}^v are SIA and vacancy bias factor of grain boundary in prism, Z_{gb}^i and Z_{gb}^v are SIA and vacancy bias factor of grain boundary in basal plane. A_{poly} is

51

anisotropy factor of interesting direction. ϵ_d is irradiation growth of interesting direction. In this paper it was assumed that grain boundary are distributed isotropic. Therefore the value of average stain factor of grain boundary has 0.5. At single crystal, bias factor was modified by DAD. However, in polycrystalline case, bias factor should be modified one more time, because of grain boundary enhanced diffusion. Unfortunately there is not research about grain boundary enhanced diffusion in irradiation situation. Therefore, the bias factor was modified at several attempt. The detail discussion had been done in result and discussion chapter.

4.3 Improved radiation-induced growth modeling results

After establishment of defect rate equation and growth strain equation, defect concentration and irradiation growth results are calculated by python code program. In this section, three case of zirconium are examined and compared with experiment data. In the modeling section polycrystalline modeling are developed just one case because polycrystalline modeling could explain both of cold work and annealed case. However, in real application region, polycrystalline should be separated as annealed and cold work case because they show much different growth result. Therefore, in this results section, growth modeling results are composed three part that single, annealed and cold worked although modeling are composed two part such as single and polycrystalline.

In case of annealed and cold worked polycrystalline, it was assumed that diffusion coefficient was higher than single crystalline case because of grain boundary enhanced mobility. However there was not general reference about grain boundary enhanced diffusion. Therefore, diffusion coefficient effect was modified by cold worked code simulation. In case of cold worked polycrystalline, irradiation growth was not well matched with experimental data. However, when diffusion coefficient modified at eight times (8.0×10^{-6}), irradiation growth result was well matched. Therefore, this diffusion coefficient was adopted in annealed polycrystalline case because annealed polycrystalline also have same grain boundary size.

The results are systemically analysis such as single, annealed and cold work case. In the each case, defect concentration and growth result are expressed. The figure of defect concentration was directly used of python code program (MATPLOT). However, in case of irradiation growth data, the figure was edited by ORIGIN program hence to compare with experiment data.

4.3.1 Single crystal zirconium

In case of single crystal, defect concentration behavior show typical row sink density behavior. The term of row sink density are coined by Gary S. Was [6]. Initially, defect concentrations is linear increasing because the concentrations are too low for either recombination or interaction with sinks. And after of point defects are build-up, recombination rate could be effect on defect concentration because recombination rate are increased by increased defect concentration. Therefore, point defect will start to be steady state at certain point because production rate is compensated with recombination rate. However, after this steady state region cause by recombination, sinks also have another loss effect on the defect concentration. As referred before, the firstly SIAs interaction with sinks and sinks will consume the point defect because SIA diffusion coefficient much faster than vacancy. Because of sink induced annihilation of SIA concentration of SIA is decreasing whilst vacancy concentration are increasing because of SIA concentration deceasing which should be recombine. Lastly, SIA concentration show steady state because SIA concentration is sufficiently row. And also vacancy also show steady state.   Fig IV.1 show defect concentration of single crystal defect concentration.
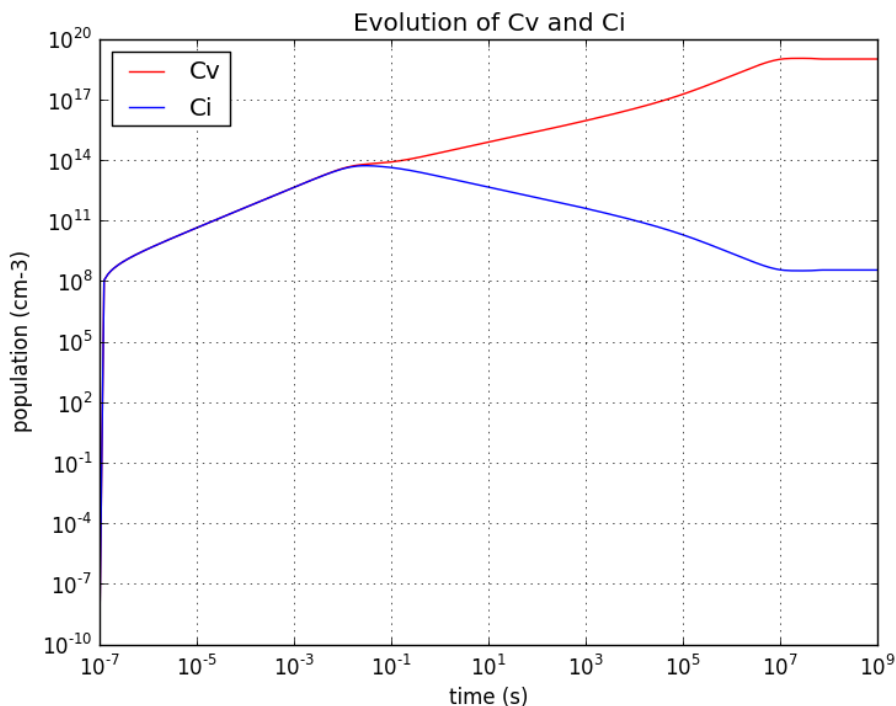
Fig IV.1 Point defect concentration in single crystal zirconium

As referred, major sink in the single crystal is dislocation loop density. Therefore, two type of loop are examined. Fig IV.2 show dislocation loop density verse dpa. At first stage both loop density are row, however, after 0.1 dpa, <a> dislocation loop are increasing dramatically and <c> type loop increasing after <3> dpa region. And after increasing region, both loop show saturation region. These behavior are exactly followed the modeling structure, which is author intended. In case of <a> dislocation loop initiation of loop increasing was automatically occurred by defect flux behavior which calculated by python code. However, in case of <c> dislocation loop initiation are considered from experiment data. Lastly, saturation behavior, also considered by experiment database.
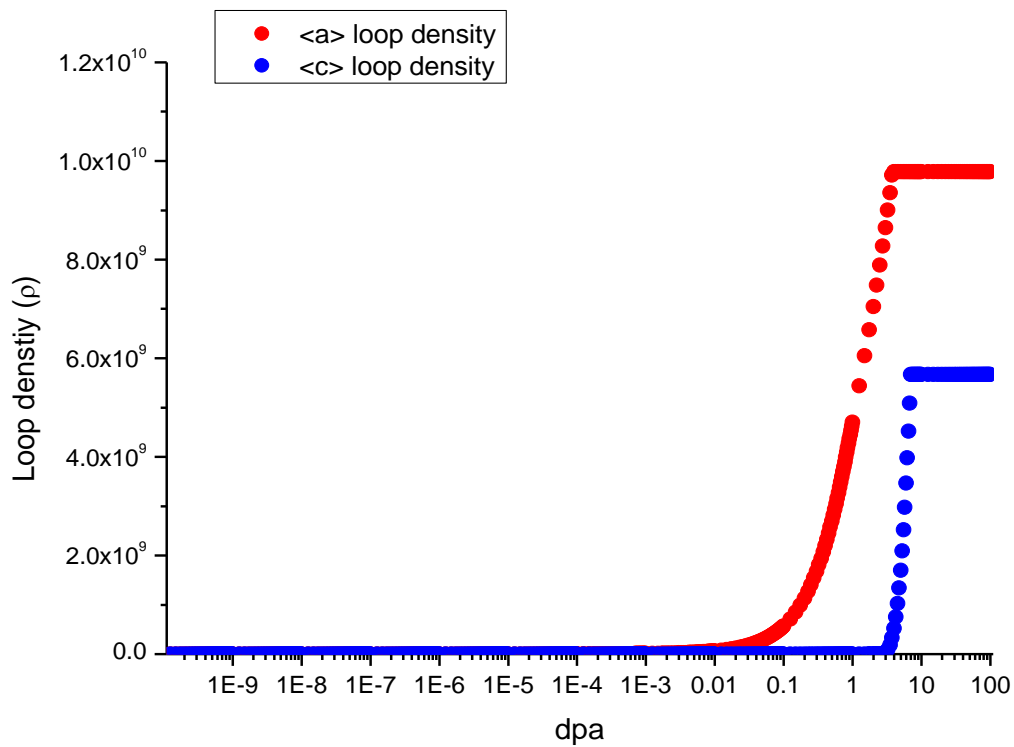
Fig IV.2 Dislocation loop behavior in the single crystal zirconium

In case of net defect flux to sink behavior, also two type of defect are analysis because major sink are dislocation loops. Fig IV.3 shows the net defect flux to sink. At first stage, net defect flux to both loop are increased and right after, decreased. Because at early stage, as referred before, SIA diffusion coefficient much faster than vacancy, net defect flux to sink are much higher than other dpa region. However, fortunately, this phenomenon is occurred during very short time and sink are not developed. Therefore, this phenomenon effect on the irradiation growth are negligible. Therefore, actual effect on the growth is occurred at steady state net flux region.
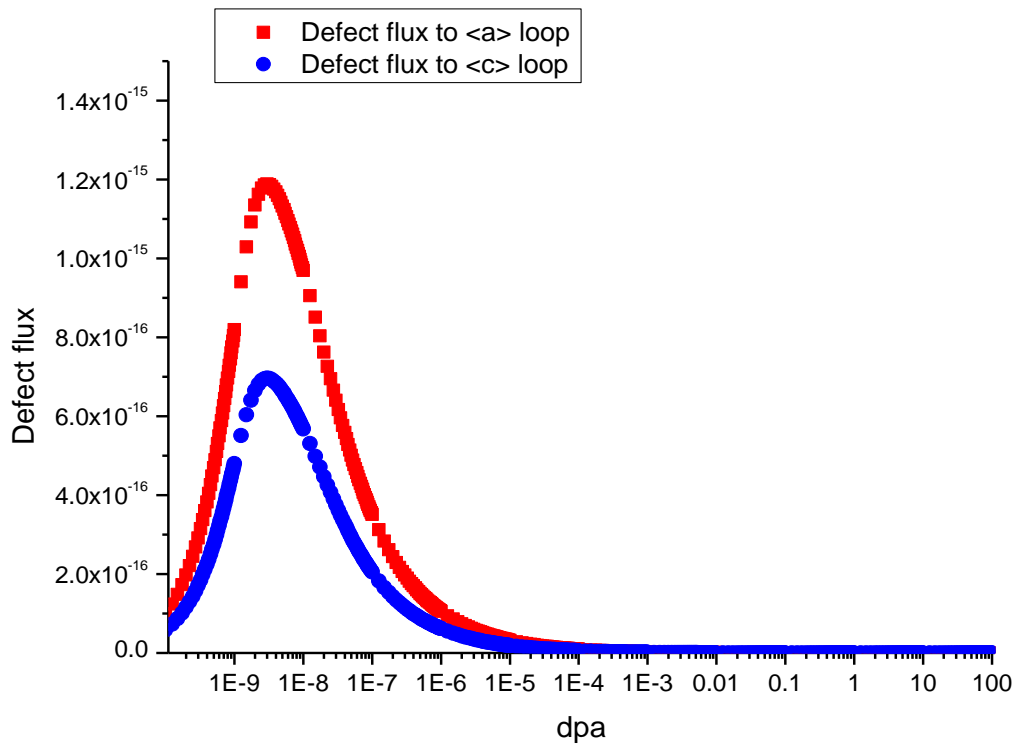
Fig IV.3 Defect flux behavior in the single crystal zirconium

From the defect concentration data, irradiation growth could be calculated. In case of single crystal. In Fig IV.4, the modeling result show break away phenomenon. As referred before, irradiation growth phenomenon was separated by three part. First stage, because of high defect flux make high growth strain. And then, growth was saturated by vacancy defect concentration increasing. Finally, growth was accelerated by <c> dislocation loop generation.
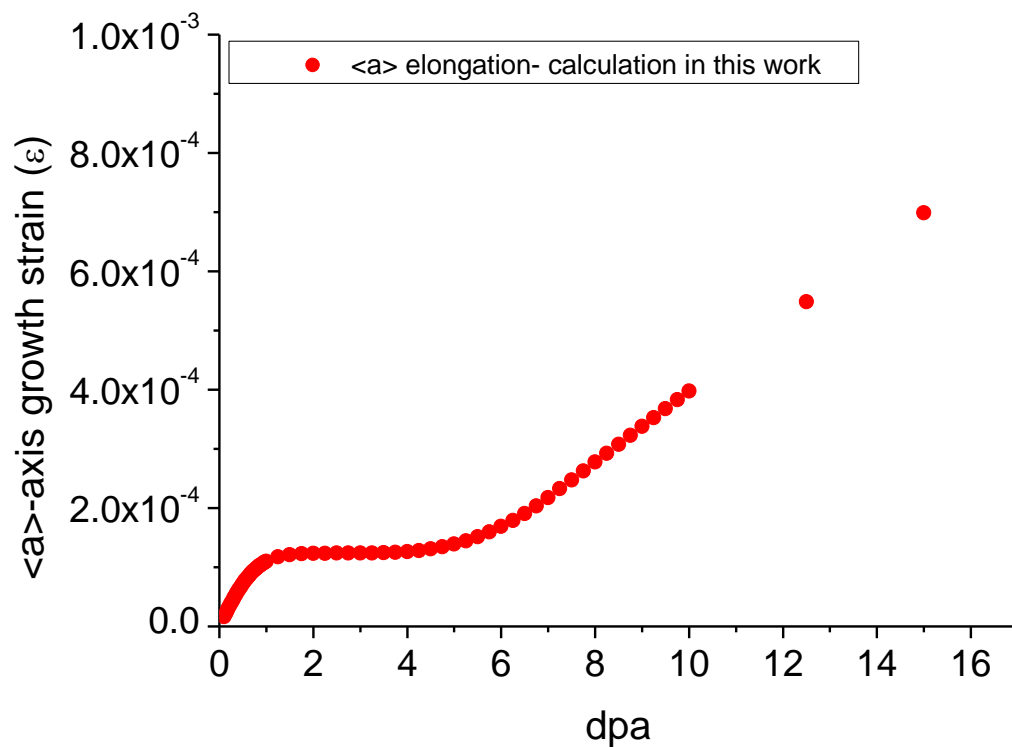
Fig IV.4 Irradiation growth strain results of single crystal zirconium

4.3.2 Annealed zirconium

In case of Annealed polycrystalline, defect concentration behavior show typical intermediate sink density behavior. The term is also coined by Gary S. Was textbook. As like single crystal case, initially, defect concentrations is linear increasing because the concentrations are too low for either recombination or interaction with sinks.

However, in this annealed polycrystalline case, after of point defects are build-up, recombination rate effect are negligible at early stage because SIA consumed firstly by sink because of increased sink density. Therefore, SIA show steady state and vacancy are increased.

After in this time, recombination effect are considerable, therefore, both of defect concentration are decreasing. And lastly, SIAs are sufficiently low, defect concentration shows shat final steady state region. In this final region, production and annihilation of recombination and sink consuming are balanced. Fig IV.5 shows defect concentration of annealed polycrystalline defect concentration.
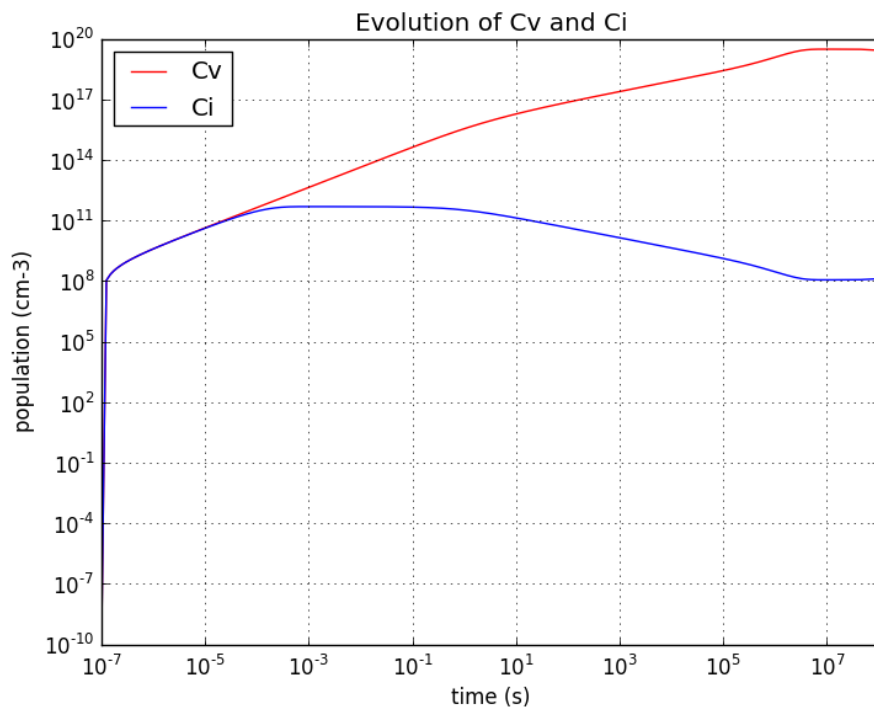
Fig IV.5 Irradiation growth strain results of annealed polycrystalline zirconium

In case of annealed polycrystalline, major sink is dislocation loop density and grain boundary. Therefore three type of sink are examined. Fig IV.6 show dislocation loop density and grain boundary behavior sink strength verse dpa. At first stage, both loop density are row, however, grain boundary sink strength have certain value (3.38×10^8). However, after 10^{-9} dpa, grain boundary sink strength are dramatically decreased close to 0 cm^{-2} at 0.1 dpa. This result is physically impossible, however, defect concentration, which was calculated in this modeling make grain boundary sink strength weaken. And after this low sink strength region, both <a> loop and grin boundary are increasing because of <a> loop generation. And after 1 dpa, <c> loop are generated and <c> loop increasing without saturation. This phenomenon is also physically impossible. Therefore. It was clear that this advanced modeling, which could be adopted in single and cold worked polycrystalline, could not be adopted in annealed polycrystalline. Therefore, the assumption for the annealed polycrystalline should be modified.

Fig IV.6 Defect flux behavior in the annealed polycrystalline zirconium

In case of net defect flux to sink behavior, also three type of defect are analysis because major sink are dislocation loops and grain boundary. Fig IV.7 shows the net defect flux to sink. As like single crystal case, sink strength are sufficiently low. Therefore At first stage, net defect flux to sink are increased and right after, decreased. And defect flux show steady state region.
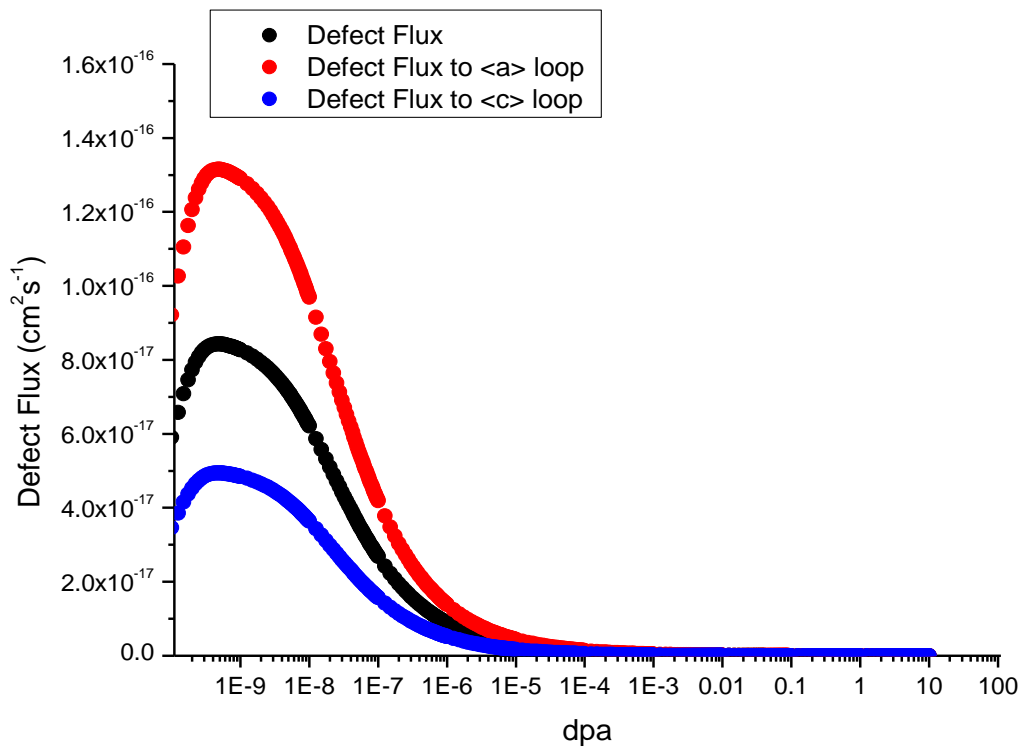
Fig IV.7 Sink density in the annealed worked polycrystalline zirconium

Fig IV. 8 shows the annealed polycrystalline growth results. The results show similar behavior with first stage of single crystal case because in case of annealed polycrystalline grain boundary play as the vacancy sink. Therefore, growth strain was higher than single crystal case. However, in case of polycrystalline, breakaway phenomenon was not occurred. Hence there was not sharply increasing of growth strain.
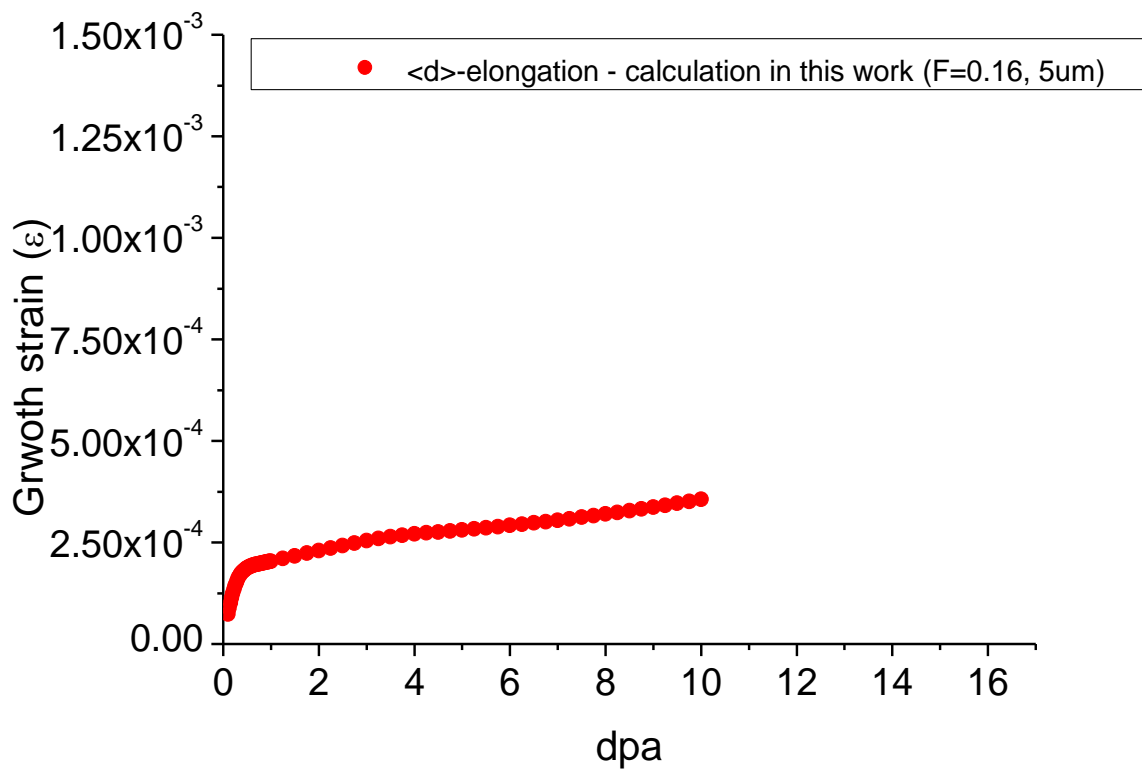
Fig IV.8 Irradiation growth strain results of annealed polycrystalline zirconium

4.3.3 Cold worked zirconium

In case of cold worked polycrystalline, defect concentration behavior show typical high sink density behavior. As like annealed polycrystalline case, initially, defect concentrations is linear increasing because the concentrations are too low for either recombination or interaction with sinks.

And also after of point defects are build-up, recombination rate effect are negligible at early stage because SIA consumed firstly by sink because of increased sink density. Therefore, SIA show steady state and vacancy are increased.

However, in case of cold worked polycrystalline case, after in this time, recombination rate effect are also negligible. Therefore, SIA concentration decreasing rate is smaller than annealed polycrystalline case, lastly as like annealed case, both of SIA and vacancy concentration are show steady state. Fig IV.9 shows defect concentration of cold worked polycrystalline defect concentration.
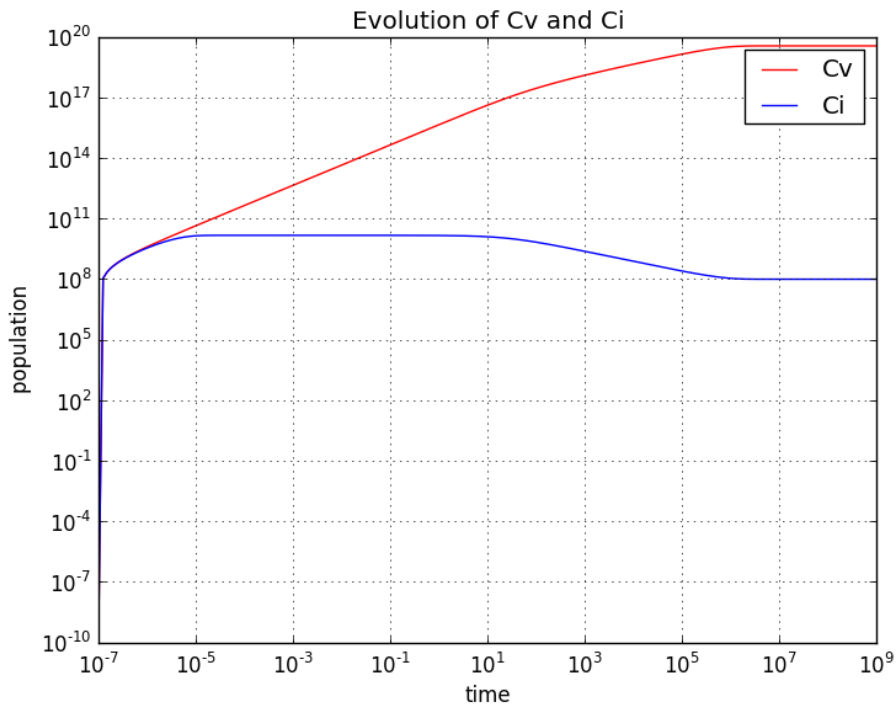
Fig IV.9 Irradiation growth strain results of cold worked polycrystalline zirconium

Because the major sink of cold worked polycrystalline is dislocation line and grain boundary therefore three type of sink are examined. Fig IV.10 shows dislocation line density and grain boundary behavior sink strength verse dpa. In case of dislocation line, it was assumed that time independent parameter. Therefore, dislocation line density are constant with dpa. Physically, cold worked zirconium, dislocation line density are already development sufficiently. Therefore, dislocation line density could not be increased because dislocation line evolve to the network dislocation. In case of grain boundary, sink strength function depend on dislocation line density. Therefore, sink strength of grain boundary also constant with dpa.
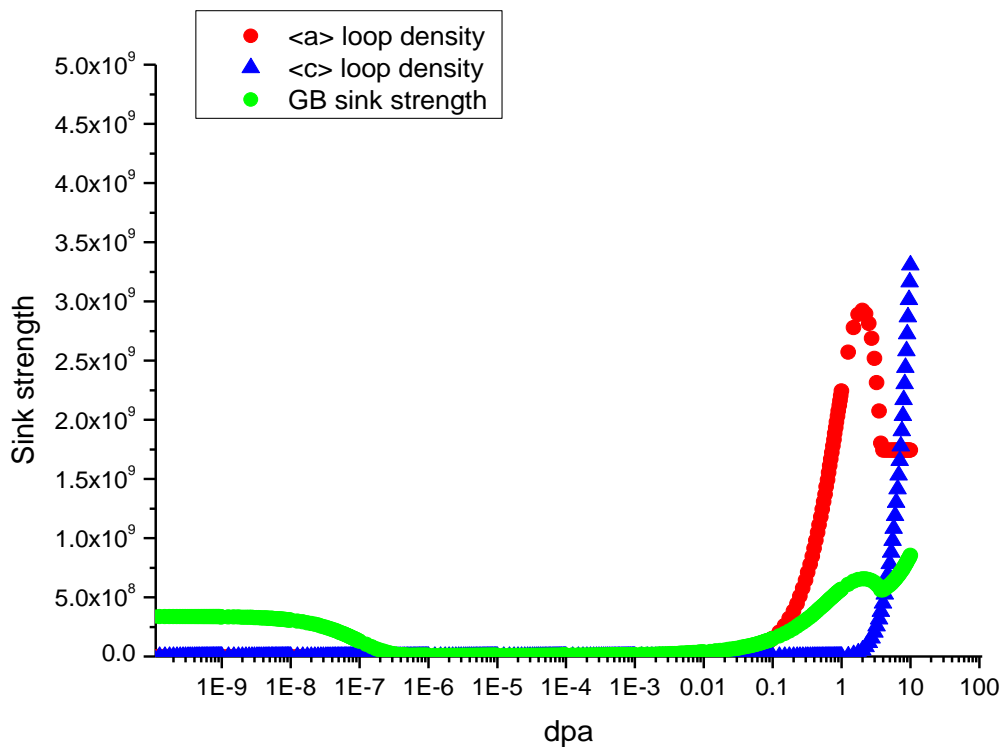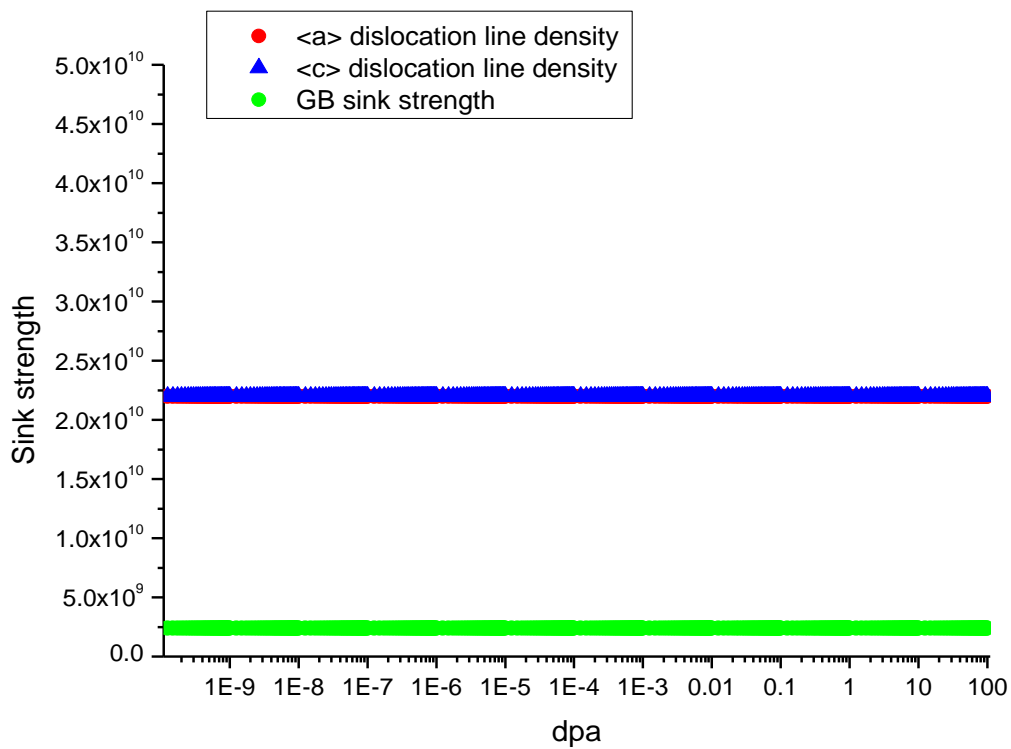

Fig IV.10 Sink density in the cold worked polycrystalline zirconium

In case of net defect flux to sink behavior, also three type of defect are analysis because major sink are dislocation line and grain boundary. Fig IV.11 shows the net defect flux to sink. Different from single crystal and annealed polycrystalline case, defect flux to sink are decrease at first stage. This phenomenon cause by high sink strength. In cold worked polycrystalline zirconium case, sink strength are highly enough to consume the defect concentration at early stage because dislocation line are already exist before the irradiation. Therefore, right after early stage, defect flux show steady state region.
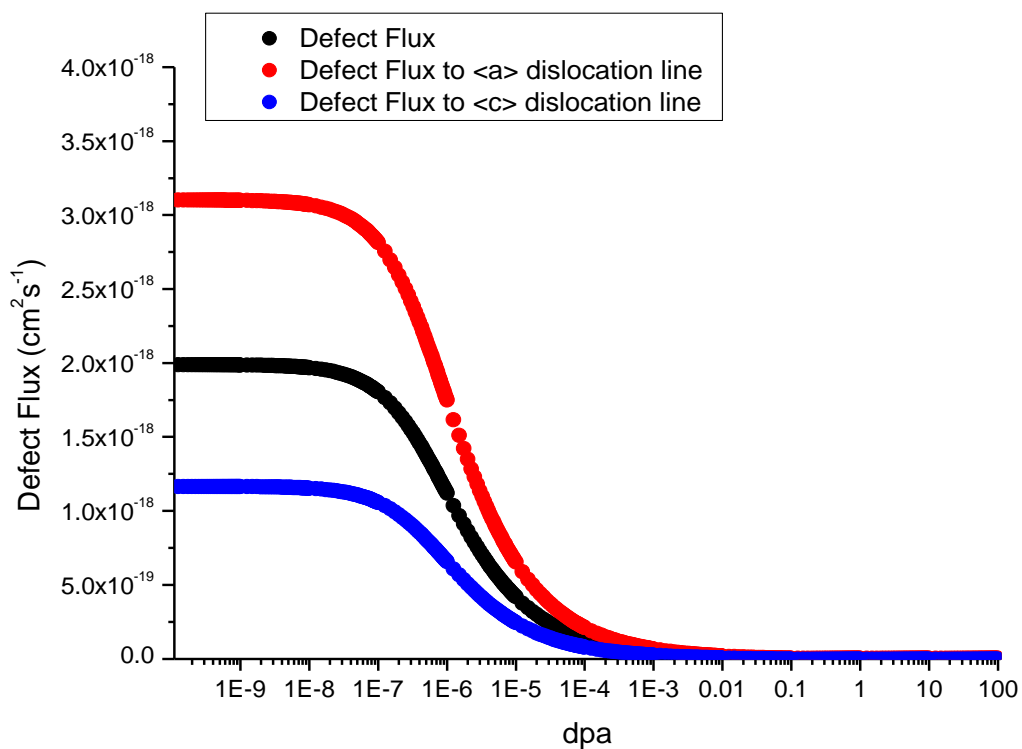
Fig IV.11 Sink density in the cold worked polycrystalline zirconium

In Fig IV.12, cold worked polycrystalline modeling results are presented. In case of cold worked polycrystalline, dislocation line sink effects are dominant. Therefore, irradiation growth is occurred with very simple behavior. Irradiation growth show linear increasing with dpa.
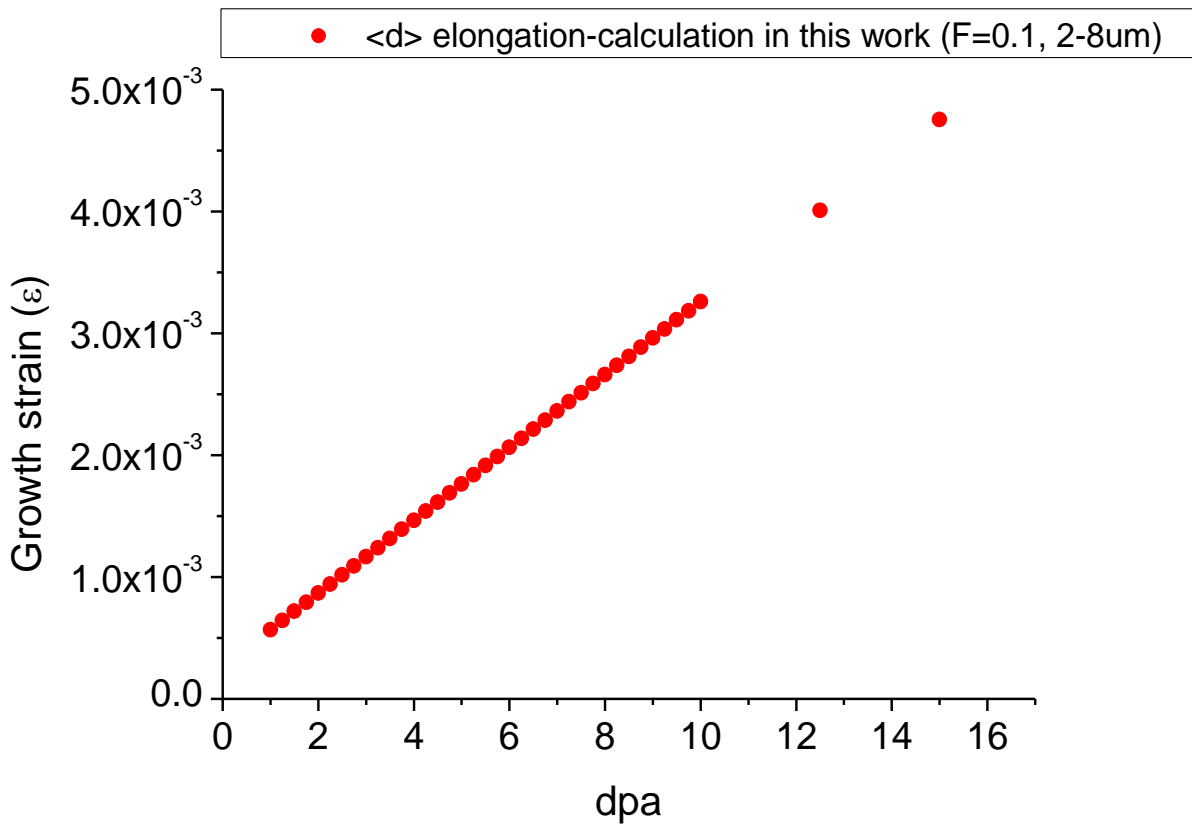
Fig IV.12 Irradiation growth strain results of cold worked polycrystalline zirconium

4.3.4 FEM modeling

As referred in introduction section, from this theoretical calculation, FEM modeling are conducted for the safety analysis. In case of ANSYS program, there is not function such as "SWELLING", which function could directly deformed material geometry without stress or temperature input data. Therefore, irradiation growth was simulated by using thermal expansion module for the simulation of materials deformation phenomenon.

The structure geometry was assumed as a guide tube in the research reactor. Specific geometry data could not be suggested because of security. Therefore, rough schematic are used such as square tube (X: 21.4 cm, Y: 21.4 cm, Z: 100. cm).

In case of environment condition, zirconium alloy was assumed cold worked, dpa 5 and 553 K. The corresponding growth strain in this environment is 0.3 %. This growth strain was simulated by thermal condition. Because of zirconium thermal expansion coefficient is about $5.0 \times 10\text{-}6$, thermal condition was given 1.7×103. And actually, irradiation growth is happened severely in middle parts. Therefore, temperature are distrusted as linear increasing (lowest 1650 ℃, highest 1700 ℃). In Fig IV.13, temperature distribution are shown.
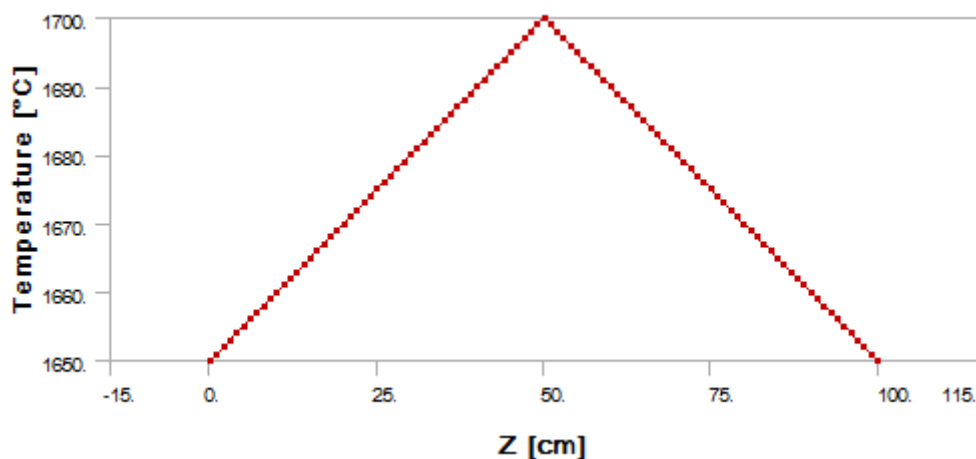
Fig IV.13 Temperature distribution by z-axis

After input data was established, specific mesh method are adopted. In case of square tube, mapped face meshing method are used for the uniform mesh distribution. And in case of fix condition, fixed support was chosen because in the actual guide tube are located with fiction less. Fig IV. 14 show mesh morphology
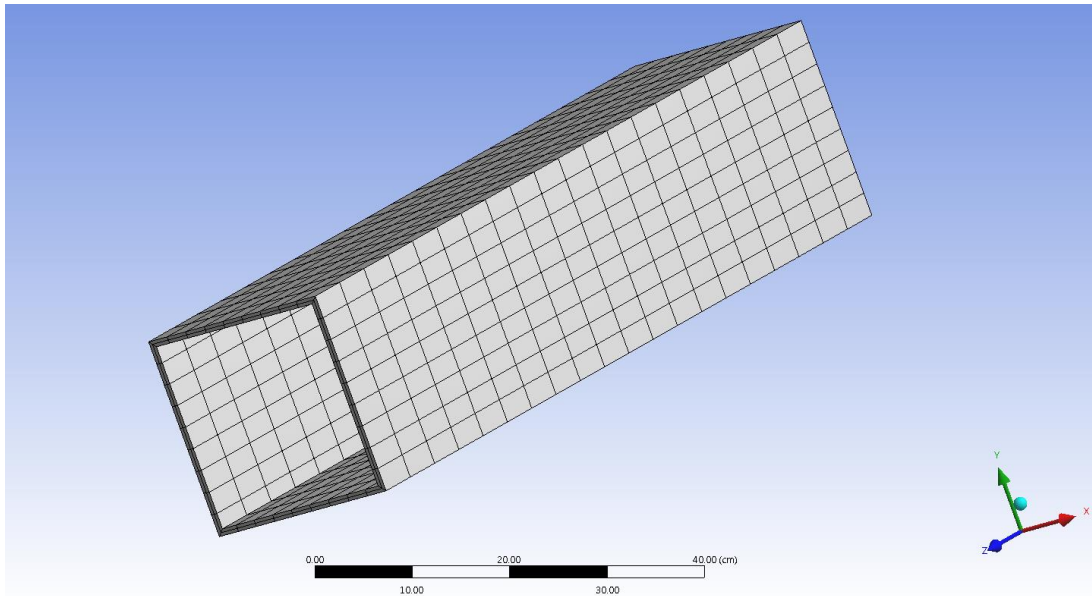
Fig IV.14 Geometry of guide structure with mapped face meshing

Eventually, equivalent elastic strain was calculated from the ANSYS modeling. At given environment, irradiation growth induced maximum 0.85% strain at guide tube. Fig IV.15 show Equivalent elastic strain of guide tube geometry. This value could be used for the safety analysis. The specific data which used in this ANSYS modeling are shown in the appendices chapter.
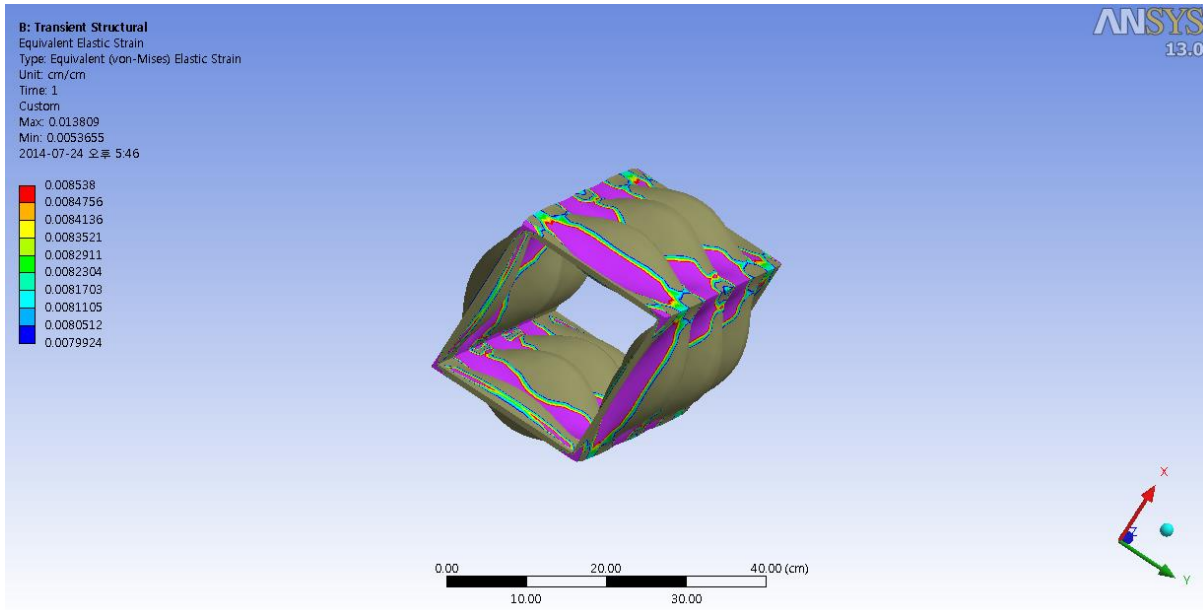
Fig IV.15 Equivalent elastic strain of guide tube geometry by irradiation growth

V.   Discussions

From the defect concentration, irradiation growth are calculated in the result chapter. In this chapter, calculation result are compare with experiment data for the verification. Therefore, the certain limitation could be evolved. Specifically, in case of single crystal, irradiation growth experiment was measurement by carpenter [13]. And the modeling results, compared with experimental data are presented in Fig V.1. The modeling results were similar to the experimental results. However, the values of the elongation between 2 ~ 6 dpa, experiment were higher than for calculation data. Form this phenomenon, it could be analyzed that dislocation sink density function is most important factor in the irradiation growth.
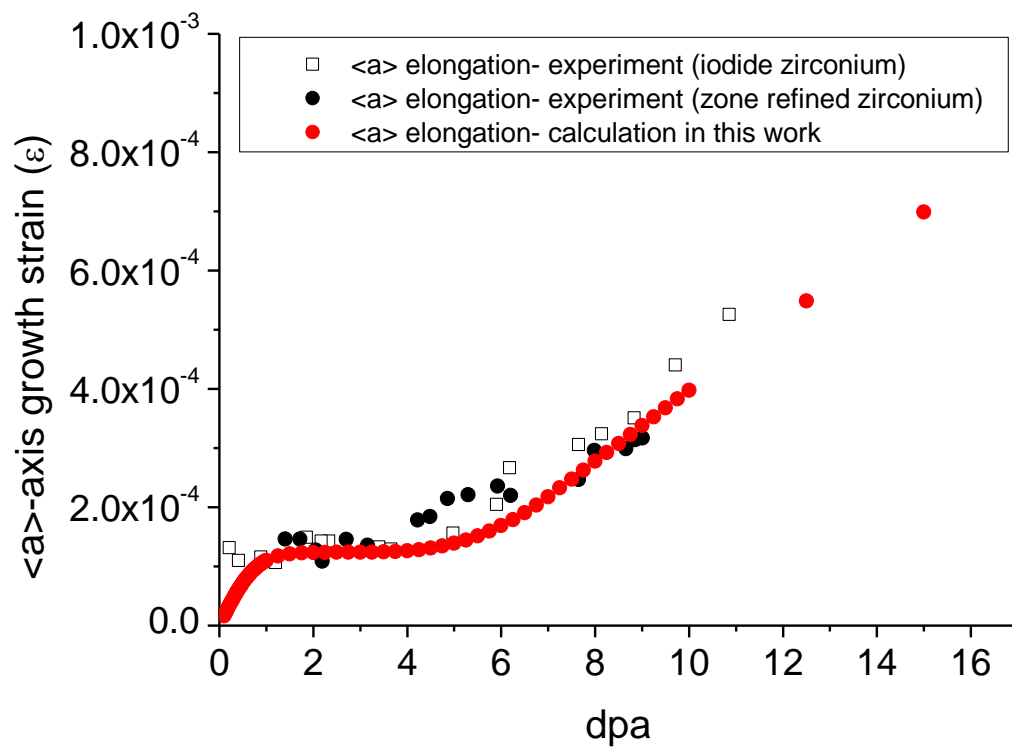
Fig V.1 Irradiation growth strain results of modeling and experiment of single crystal zirconium [13]

Fig V.2 shows the annealed polycrystalline growth results, which are compared with experimental data [16]. Both results of experiment and modeling show high growth strain at the beginning. However, after 1 dpa, calculated strain show much lower increasing behavior. This difference behavior are increased with increasing dpa. From the sink strength data, it could be analyzed that grain boundary sink strength and <a>, <c> dislocation loop are reason of this disagreement behavior. In case of grain boundary, the sink strength model base on the dislocation loop density and dislocation density model base on the defect rate equation. Therefore, the final conclusion of annealed polycrystalline case is new mechanism of defect rate equation for the grain boundary should be suggested. Unfortunately there is not general modeling about grain boundary sink strength or heterogeneous defect rate equation for the grain boundary. Apart from general equation, several parameter are also could be reason of this disagreement behavior. In case of diffusion coefficient, many author depend on the theirs computer simulation result. Unfortunately, The result of many author's computer simulation are different each other and also different form the experimental result. Therefore, diffusion coefficient should be verified by fundamental research.
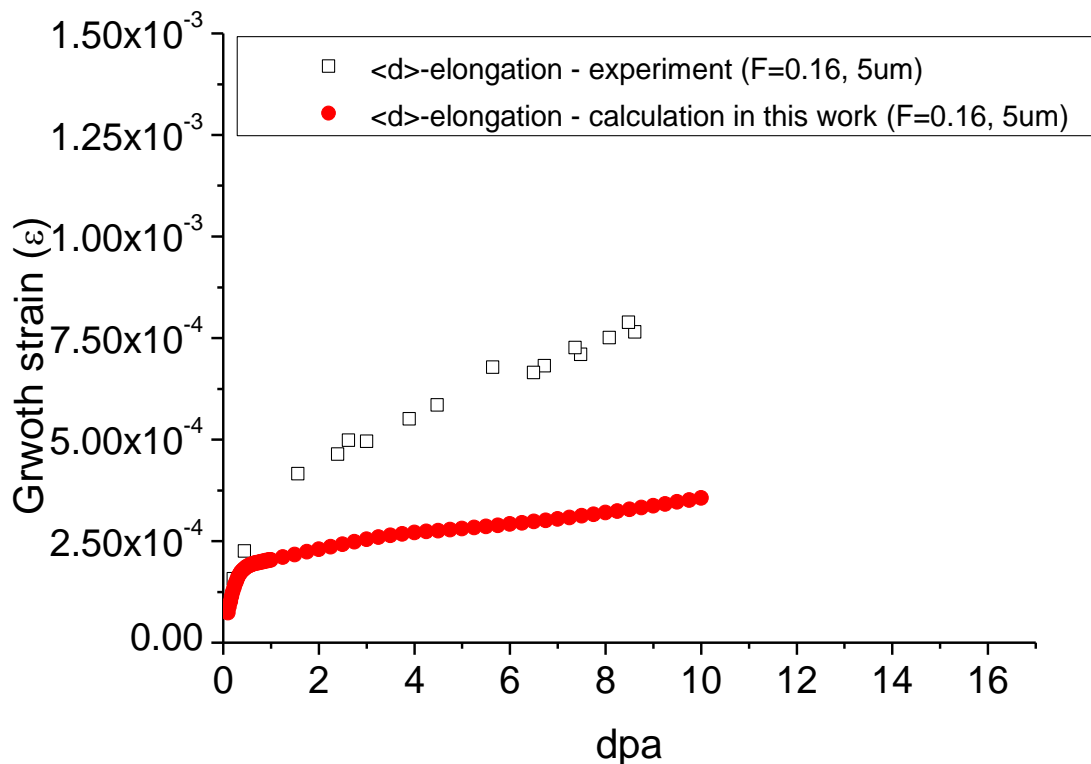
Fig V.2 Irradiation growth strain results of modeling and experiment of annealed polycrystalline zirconium [16]

In Fig V.3, the modeling results present quite similar growth strain value as compared to experimental results [16]. Both theoretical and experimental data show a linear increase. In the case of the cold-worked polycrystalline sample, the results were compared to experimental data of cold-worked zircaloy because there is an absence of cold-worked polycrystalline reference data. Fortuitously, most of the research has assumed that the alloy element effect is negligible since the dislocation line sink effects are so dominant.
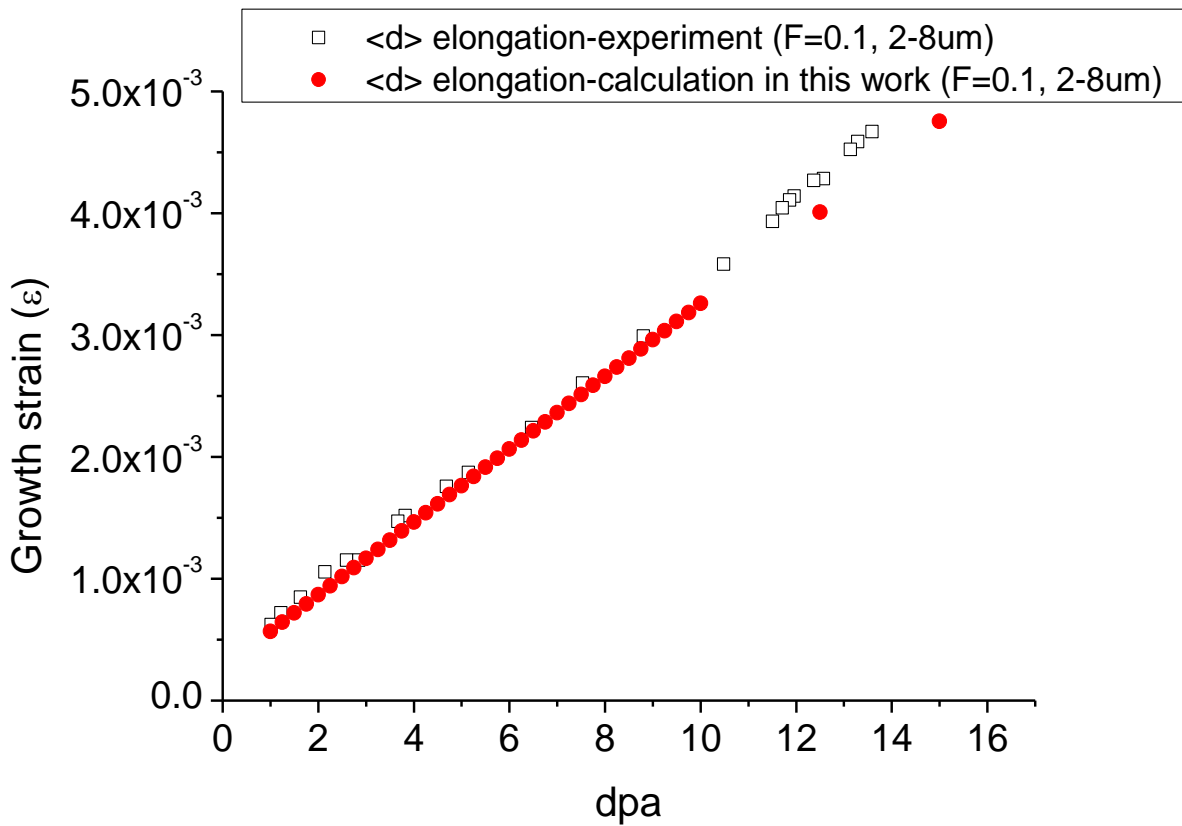
Fig V.3 Irradiation growth strain results of modeling and experiment of cold worked polycrystalline zirconium [16]

Irradiation growth is one of the most important phenomenon in the nuclear safety analysis. However there was not general irradiation growth modeling of polycrystalline for various temperature region. Therefore this work is very important for the nuclear safety analysis. However growth modeling is very difficult because it should be combined that defect rate equation and irradiation growth strain equation. Both of defect rate equation and irradiation growth strain modeling are not easy to establish because in order to realistic modeling, we should consider various parameter such as diffusion coefficient, sink strength, capture efficiency, and anisotropy factor. From these parameters, growth result could be modified

Although, these toughness, historically defect rate equation are developed by many researchers. In 1993, Holt [6] explain PBM effects on the zirconium metal. From this assumption, experiment result are well matched with irradiation growth modeling form research reactor to commercial reactor temperature. PBM framework could explain discrepancy between modeling and experiment. However, in this paper, defect rate equation consider only point defect because cluster effect was consider as dislocation loop. From this assumption, irradiation growth are calculated. May be absence of PBM assumption could be reason of disagreement of annealed polycrystalline case. And also development of dislocation loop could be one reason. Grain boundary sink strength are also one reason of disagreement result. However, in these days, there was not general theory and simulation result about sink strength. Therefore, fundamental analysis is needed for the understanding about irradiation growth behavior.

In the results chapter, defect concentration, defect flux, sink strength and irradiation growth strain results are explain. From the results, it could know that actually irradiation growth strain are determined by net defect concentration at final steady state region. Therefore, lastly, it is clear that irradiation growth are depended sink strength. Therefore, detail analysis of irradiation growth, sink strength and defect flux are examined each case such as single crystal, annealed and cold worked polycrystalline. From these results, it was confirm that it is hard to predict growth strain of annealed polycrystalline because there are many parameter which should be verified such as diffusion coefficient, grain boundary sink strength, assumption of defect rate equation and <c> dislocation shortening effect.

Unfortunately, annealed polycrystalline result was well matched with experiment result. However, from the result of single crystal and annealed polycrystalline case, it was confirm that major sink strength change and defect flux behavior in the result and discussion chapter in detail.

Therefore, it could be analyzed that grain boundary sink strength and general defect rate equation are not adopted in annealed polycrystalline case. In case of defect rate equation, assumption of defect rate

equation should be extended to cluster and point defect clustering modeling should be implementation. These modeling technic for the defect rate equation must come with high cod programing skill.

1. Therefore, in the next research stage, defect rate equation will be developed by python code program in order to reflect real irradiation situation.

2. In case of grain boundary sink strength, the theoretical study about physical chemistry should be done in firstly. And then computer simulation could be guide of sink strength modeling. Therefore, MD simulation will be conducted for the precisely prediction modeling.

3. In case of the irradiation growth strain equation, <c> axis shortening phenomenon is not consider in this modeling results. Therefore, in the next research stage, <c> axis shortening will be considered. May be the new mechanism should be established because there was not general mechanism and modeling.

4. Lastly, from the polycrystalline case, it was clear that diffusion coefficient is most important parameter in the modeling. Therefore, diffusion coefficient will be treated.

VI. Summary and Conclusion

Zirconium and zirconium alloys are widely extensively used as nuclear core material. Irradiation growth phenomenon is main concern of zirconium degradation. However, in these days, there was not general modeling of irradiation growth cause its complexity of irradiation growth. Therefore, in this paper, irradiation growth modeling are conducted for the safety analysis. For the precisely analysis, various literature study had been done in experimental results and theoretical results. From the experimental results, the general characteristic of irradiation growth are understanding such as proportion behavior (fluence, temperature and texture). And from the theoretical modeling study, the defect flux and sink density and size distribution could be analyzed. After understanding of both part, the irradiation growth mechanism and govern equation are established.

The equations are set up in two case such as single crystal and polycrystalline. In case of polycrystalline, grain boundary sink effect are considered in addition to single crystal sink strength. Explain in detail about method of establishment of irradiation growth modeling. Defect rate equation are established from single crystal to polycrystalline in order to understanding of grain boundary effect. In case of dislocation loop [33] and grain boundary sink, sink strength modeling are followed recent method. Dislocation loop and grain boundary sink strength was time dependent and dislocation line and is constant. Also each sink are separated into two term by axis direction because of DAD effect on the sink strength. The one is parallel with <c> direction and second is parallel with <a> direction. Especially, grain boundary sink was assumed that isotropic morphology therefore, strength is divided equally two part. This was not never had been before. From this approach, defect concentration are calculated. After defect rate equation are established, the equation of irradiation growth strain are established. The growth strain equation is composed with sink strength and defect flux and anisotropy factor because the irradiation growth is occurred by defect accumulation by defect flux at unit sink. In case of anisotropy factor, which is induced each grain boundary orientation, are only considered in polycrystalline, because in case of single crystal, elongation occur in uniform direction. The anisotropy factor is obtained by experiment database. Also, growth strains are calculated by each sink type. Therefore, each sink induced irradiation growth could be analysis and confirm that major sink effect of growth.

Although, polycrystalline modeling are establish just one case, the modeling result are conducted in two part because cold worked and annealed polycrystalline behavior are much different. Explain in detail about irradiation growth result from the modeling in this paper.

1. In case of single crystal and cold worked polycrystalline, the result are well matched with experimental result. From the analysis of behavior of the defect flux and sink strength behavior, it was clear that the growth modeling are well established.

2. However, in case of annealed polycrystalline case, irradiation growth result not well matched with experimental results. Because in case of polycrystalline case, the sink behavior are more complex than single and cold worked case. Therefore, in case of polycrystalline case, the other parameter such as diffusion coefficient and grain boundary sink strength should be analyzed more fundamentally.

VII. Reference

[1]   M. Griffiths, "Evolution of microstructure in hcp metals during irradiation," *Journal of Nuclear Materials,* vol. 205, pp. 225-241, // 1993.

[2]   C. H. Woo, "DISLOCATION BIAS IN AN ANISOTROPIC DIFFUSIVE EDIUM AND IRRADIATION GROWTH," *Journal of Nuclear Materials,* vol. 119, pp. 219-228, 1983.

[3]   W. Frank, "Intrinsic point defects in hexagonal close-packed metals," *Journal of Nuclear Materials,* vol. 159, pp. 122-148, 10// 1988.

[4]   Y. N. Osetsky, D. J. Bacon, and N. De Diego, "Anisotropy of point defect diffusion in alpha-zirconium," *Metallurgical and Materials Transactions A: Physical Metallurgy and Materials Science,* vol. 33, pp. 777-782, // 2002.

[5]   R. C. Pasianot and A. M. Monti, "A many body potential for α-Zr. Application to defect properties," *Journal of Nuclear Materials,* vol. 264, pp. 198-205, // 1999.

[6]   G. S. Was, "fundamentals of radiation materiasl science," 2007.

[7]   J. L. Straalsund, R. W. Powell, and B. A. Chin, "An overview of neutron irradiation effects in LMFBR materials," *Journal of Nuclear Materials,* vol. 108–109, pp. 299-305, 7// 1982.

[8]   C. H. Woo, "THEORY OF IRRADIATION DEFORMATION IN NON-CUBIC METALS effects of anisotropic diffusion," *Journal of Nuclear Materials,* vol. 159, pp. 237-256, 1988.

[9]   S. N. Buckley, "Properties of reactor materials and effects of irradiation damage", p. 413, 1962.

[10]   V. Fidleris, "Summary of experimental results on in reactor creep and irradiation growth of zirconium alloys," *ATOM.ENERGY REV,* vol. 13, pp. 51-80, // 1975.

[11]   R. B. Adamson, *zirconium in the nuclear industry,* vol. ASTM 633 p. 326, 1977.

[12] G. J. C. CARPENTER, R. A. MURGATROYD, A. ROGERSON, and J. F. WATTERS, "Irradiation growth of zirconium single crystals," *Journal of Nuclear Materials,* vol. 1981, pp. 28-37, 1981.

[13] G. J. C. CARPENTER, R. H. ZEE, and A. ROGERSON, "IRRADIATION GROWTH OF ZIRCONIUM SINGLE CRYSTALS A REVIEW," *Journal of Nuclear Materials,* vol. 159, pp. 86-100, 1988.

[14] V. FIDLERIS, "The irradiation creep and growth phenomena," *Journal of Nuclear Materials,* vol. 159, pp. 22-42, 1988.

[15] R. A. MURGATROYD and A. ROGERSON, "IRRADIATION GROWTH IN ANNEALED ZIRCALOY-2," *Journal of Nuclear Materials,* vol. 79, pp. 302-311, 1979.

[16] A. ROGERSON, "IRRADIATION GROWTH IN ZIRCONIUM AND ITS ALLOYS," *Journal of Nuclear Materials* 1988.

[17] A. ROGERSON, "IRRADIATION GROWTH IN ANNF,ALED AND 25% COLD-WORKED ZIRCALOY-2 BETWEEN 353 - 673 K," *Journal of Nuclear Materials,* vol. 154, pp. 276-285, 1988.

[18] A. ROGERSON, "IRRADIATION GROWTH IN ZIRCONIUM-TIN ALLOYS AT 353 AND 553 K," *Journal of Nuclear Materials,* vol. 152, pp. 220-224, 1988.

[19] A. ROGERSON and R. A. MURGATROYD, "EFFECTS OF TEXTURE AND TEMPERATURE CYCLING ON IRRADIATION GROWTH IN COLD-WORKED ZIRCALOY-2 AT 353 and 553 K," *Journal of Nuclear Materials,* vol. 80, pp. 253-259, 1979.

[20] A. Rogerson and R. A. Murgatroyd, "'BREAKAWAY' GROWTH IN ANNEALED ZIRCALOY-2 AT 353 K AND 553 K," *Journal of Nuclear Materials,* vol. 113, pp. 256-259, 1983.

[21] A. ROGERSON and R. H. ZEE, "HIGH FLUENCE IRRADIATION GROWTH IN SINGLE CRYSTAL ZIRCONIUM AT 553 K," *journal of Nuclear Materials,* vol. 151, pp. 81-83, 1987.

[22]   R. H. ZEE, G. J. C. CARPENTER, A. ROGERSON, and J. F. WAtTERS, "IRRADIATION
        GROWTH IN DEFORMED ZIRCONIUM," *Journal of ASTM international,* vol. 150, pp.
        319-330, 1987.

[23]   R. A. Holt, "In-reactor deformation of cold-worked Zr–2.5Nb pressure tubes," *Journal
        of Nuclear Materials,* vol. 372, pp. 182-214, 2008.

[24]   R. A. Holt, "In-Reactor Deformation of Zirconium Alloy Components," *Journal of
        ASTM international,* vol. STP 1505, 2008.

[25]   R. A. Holt, G. A. Bickel, and N. Christodoulou, "Effect of fast neutron fluence on the
        creep anisotropy of Zr–2.5Nb tubes," *Journal of Nuclear Materials,* vol. 373, pp. 130-
        136, 2008.

[26]   R. A. Holt, M. R. Daymond, F. Xu, and S. Cai1, "Intergranular and Interphase
        Constraints in Zirconium alloy," *Journal of ASTM international,* 2008.

[27]   M. A. McGrath, S. Yagnik, P. Barberis, and S. W. Dean, "Experimental Investigation of
        Irradiation Creep and Growth of Recrystallized Zircaloy-4 Guide Tubes Pre-Irradiated
        in PWR," *Journal of ASTM International,* vol. 8, p. 103770, 2011.

[28]   M. GRIFFITHS, "A review of microstructure evolution in zirconium alloys during
        irradiation," *Journal of Nuclear Materials,* vol. 159, pp. 190-218, 1988.

[29]   R. A. Holt, "EFFECT OF MICROSTRUCTURE ON IRRADIATION CREEP AND GROWTH
        OF ZIRCALOY PRESSURE TUBES IN POWER REACTORS," *Journal of Nuclear Materials,*
        vol. 82, pp. 419-429, 1979.

[30]   R. A. Holt, "ANISOTROPY OF IRRADIATION CREEP AND GROWTH OF ZIRCONIUM
        ALLOY PRESSURE TUBES," *Journal of Nuclear Materials,* vol. 91, pp. 311-321, 1980.

[31]   R. A. Holt, "Mechanisms of irradiation growth of alpha-zirconium alloys," *Journal of
        Nuclear Materials,* vol. 159, pp. 310-338, 1988.

[32]   F. Christien and A. Barbu, "Cluster Dynamics modelling of irradiation growth of
        zirconium single crystals," *Journal of Nuclear Materials,* vol. 393, pp. 153-161, 2009.

[33] S. I. Golubov, A. V. Barashev, and R. R. Stoller, "ON THE ORIGIN OF RADIATION GROWTH OF HCP CRYSTALS," *ONRL,* 2011.

[34] F. Onimus and J. L. Béchade, "4.01 - Radiation Effects in Zirconium Alloys," in *Comprehensive Nuclear Materials*, R. J. M. Konings, Ed., ed Oxford: Elsevier, 2012, pp. 1-31.

[35] R. Sizmann, "The effect of radiation upon diffusion in metals," *Journal of Nuclear Materials,* vol. 69-70, pp. 386-412, // 1978.

[36] M. Kiritani, "Microstructure evolution during irradiation," *Journal of Nuclear Materials,* vol. 216, pp. 220-264, 1994.

[37] K. Farrell, T. S. Byun, and N. Hashimoto, "Deformation mode maps for tensile deformation of neutron-irradiated structural alloys," *Journal of Nuclear Materials,* vol. 335, pp. 471-486, 2004.

[38] C. A. English, W. V. Green, M. Guinan, A. Horsewell, S. Ishino, B. N. Singh*, et al.,* "Summary of silkeborg workshop on "Radiation damage correlation for fusion conditions"," *Journal of Nuclear Materials,* vol. 174, pp. 352-354, // 1990.

[39] http://www.oecd-nea.org/tools/abstract/detail/psr-0263/.

[40] R. V. Hesketh, "Non-linear growth in zircaloy-4," *Journal of Nuclear Materials,* vol. 30, pp. 219-221, 4// 1969.

[41] G. J. C. Carpenter and D. O. Northwood, "The contribution of dislocation loops to radiation growth and creep of Zircaloy - 2," *Journal of Nuclear Materials,* vol. 56, pp. 260-266, 6// 1975.

[42] C. C. Dollins, "In-pile dimensional changes in neutron irradiated zirconium base alloys," *Journal of Nuclear Materials,* vol. 59, pp. 61-76, 1// 1976.

[43] D. FAINSTEIN-PEDRAZA, E. J. SAWNO, and A. J. PEDRAZA, "IRRADIATION-GROWTH OF ZIRCONIUM-BASE ALLOYS," *Journal of Nuclear Materials,* vol. 73, pp. 151-168, 1978.

[44] S. R. MacEWEN and G. J. C. CARPENTER, "Calculations of irradiation growth in zirconium," *Journal of Nuclear Materials,* vol. 90, pp. 108-132, 1980.

[45] R. BULLOUGH and M. H. WOOD, "MECHANISMS OF RADIATION INDUCED CREEP AND GROWTH," *journal of Nuclear Materials,* vol. 90, pp. 1-21, 1980.

[46] R. B. adamson, "Irradiation Embrittlement and Creep in Fuel Cladding and Core Components," *British Nuclear Energy Society,* p. p. 305, 1972.

[47] V. F. R.B. Adamson, "Summary of Experimental Results on In-Reactor Creep and Irradiation Growth of Zirconium Alloys," *Atomic Energy Review.*

[48] R. V. Hesketh, "Non-linear growth in zircaloy-4," *Journal of Nuclear Materials,* vol. 30, pp. 219-221, 1969.

[49] P. H. Kreyns and M. W. Burkart, "Radiation-enhanced relaxation in Zircaloy-4 and Zr/2.5 wt % Nb/0.5 wt % Cu alloys," *Journal of Nuclear Materials,* vol. 26, pp. 87-104, 1968.

VIII.   Appendices

8.1 Single crystal python code structure

```
import math as m
from numpy import *
from scipy.integrate import odeint
import matplotlib.pyplot as plt
plt.ion()



## Constant
TWO_PI = 2. * pi



## Parameter setting
# Model parameter, ODE 계산중 변화하지 않음

K0 = 4.3e15              # 1/s/cm3, Defect Generation
Kiv = 1.256e-12          # cm2/s, Interstitial and Vacancy Recombination
Dv = 3.e-17              # cm2/s, Vacancy Diffusion Coefficient
Di = 1.0e-6              # cm2/s, Interstitial Diffusion Coefficient
DLp = 5.e6               # 1/cm2, Initial Dislocation line Density at Prism Plane
DLb = 5.e6               # 1/cm2, Initial Dislocation line Density at Basal Plane
BV = 3.23e-8             # cm, Bugers Vector
Zvdp = 1.                # Constant, Bias Factor at Dislocation line in Prism Plane
Zidp = 1.56              # Constant, Bias Factor at Dislocation line in Prism Plane
Zvdlp = 1.               # Constant, Bias Factor at Dislocation loop in Prism Plane
Zidlp = 1.               # Constant, Bias Factor at Dislocation loop in Prism Plane
Zvdb = 1.                # Constant, Bias Factor at Dislocation line in Basal Plane
Zidb = 0.586             # Constant, Bias Factor at Dislocation line in Basal Plane
Zvdlb = 1.               # Constant, Bias Factor at Dislocation loop in Basal Plane
Zidlb = 0.586            # Constant, Bias Factor at Dislocation loop in Basal Plane
Zvgp = 1.                # Constant, Bias Factor at Grain Boundary in Prism Plain
Zigp = 1.56              # Constant, Bias Factor at Grain Boundary in Prism Plain
Zvgb = 1.                # Constant, Bias Factor at Grain Boundary in Basal Plain
Zigb = 0.586             # Constant, Bias Factor at Grain Boundary in Basal Plain
```

```python
## Model2,
def dF_dt2(C, t=0):
    """ Return the growth rate of Ci and Cv. """
    Ci, Cv, Si, Sv, Ni, Nv, ri, rv, DLi, DLv, dpa, Ga, DF = C



    # dpa relation with time
    ddpa_dt = 1e-7



    # <a> Loop Number Density in Prism plane
    if 0. <= dpa <= 3.8:
        dNi_dt = 2.6e7 # 1/cm3/s
    else:
        dNi_dt = 0.



    # <c> Loop Number Density in Basal plane
    if 0. <= dpa <= 3.0:
        dNv_dt = 0.
    elif 3.0 < dpa < 7.0:
        dNv_dt =   1e7#1e7 * (exp(1 * ((dpa - 1)/10)) - 1)/(exp(1) - 1) # 1/cm3/s
    else:
        dNv_dt = 0.



    # <a> Loop Ridius in Prism Plane
    dri_dt = sqrt(Si / (pi * BV * Ni)) - ri
    ri = sqrt(Si / (pi * BV * Ni)) # cm



    # <c> Loop Ridius in Basal Plane
    drv_dt = sqrt(Sv / (pi * BV * Nv)) - rv
    rv = sqrt(Sv / (pi * BV * Nv)) # cm
```

\<a\> Loop Defect Number in Prism plane

dSi_dt = TWO_PI * ri * Ni * (Di * Ci / (4.3e22) - Dv * Cv / (4.3e22))   # 1/s

if dpa <= 3.8:

    dSi_dt = dSi_dt

else:

    dSi_dt = 0.

\<c\> Loop Defect Number in Prism plane

dSv_dt = TWO_PI * rv * Nv * (Zvdb * Dv * Cv / (4.3e22) - Zidb * Di * Ci / (4.3e22))   # 1/s

if dpa <= 1.0:

    dSv_dt = 0.

elif 1 < dpa <= 7.0:

    dSv_dt = dSv_dt

else:

    dSv_dt = 0.

Dislocation line & Loop Density

dDLi_dt = TWO_PI * ri * Ni - DLi

DLi = TWO_PI * ri * Ni

dDLv_dt = TWO_PI * rv * Nv - DLv

DLv = TWO_PI * rv * Nv

TDp = DLp + DLi   # 1/cm2, Total Dislocation Density in Prism plane

TDb = DLb + DLv   # 1/cm2, Total Dislocation Density in basal plane

TD = TDp + TDb   # 1/cm2, Total Dislocation Density

Defect Concentration in Cubic per cm3

dCi_dt = K0 - Kiv * Ci * Cv - Zidlp * Di * Ci * TDp - Zidb * Di * Ci * TDb # cm3/s

dCv_dt = K0 - Kiv * Ci * Cv - Zvdlp * Dv * Cv * TDp - Zvdb * Dv * Cv * TDb # cm3/s

```
    # <a> Axis Growth stain
    dGa_dt = 0.5 * TDp * (Di * Ci / (0.43e23) - Dv * Cv / (0.43e23)) # 1/s



    # Defect Flux
    dDF_dt = 0# Di * dCi_dt * 0.500 - Dv * dCv_dt * 5.00



    return  dCi_dt,  dCv_dt,  dSi_dt,  dSv_dt,  dNi_dt,  dNv_dt,  dri_dt,  drv_dt,  dDLi_dt,  dDLv_dt,
ddpa_dt, dGa_dt, dDF_dt



t = []
exponent_start = -7
exponent_stop = 9
for exponent in range(exponent_start, exponent_stop):
    for mantissa in arange(1, 10, 0.25):
        t.append(mantissa * 10 ** exponent)
t.append(1. * 10 ** exponent_stop)
t = array(t)



## Model2 Integration
# Initial value for Model2
C0 = array([1e-10,          # Ci0
            1e-10,          # Cv0
            1e-10,          # Si0
            1e-10,          # Sv0
            1e12,           # Ni0
            1e12,           # Nv0
            1e-20,          # ri0
            1e-20,          # rv0
            1e-10,          # DLi0
            1e-10,          # DLv0
            0,              # dpa0
```

```
        0,              # dGa0
        0.])            # DF0



# Integration for Model2
C, infodict = odeint(dF_dt2, C0, t, full_output=True)
print infodict['message']



## Data resolve
Cis = C[:,0]
Cvs = C[:,1]
Sis = C[:,2]
Svs = C[:,3]
Nis = C[:,4]
Nvs = C[:,5]
ris = C[:,6]
rvs = C[:,7]
DLis = C[:,8]
DLvs = C[:,9]
dpas = C[:,10]
Gas = C[:,11]
DFs = C[:,12]



## Data print
print "%-10s    %-10s    %-10s    %-10s    %-10s    %-10s    %-10s    %-10s    %-10s    %-10s    %-10s    %-10s    %-10s" % ("dpa", "Cis", "Cvs", "Sis", "Svs", "Nis", "Nvs", "ris", "rvs", "DLis", "DLvs", "Gas", "DFs")
print 5 * "============================"
for i, v in enumerate(dpas):
    print
"%10.4e    %10.4e    %10.4e    %10.4e    %10.4e    %10.4e    %10.4e    %10.4e    %10.4e    %10.4e    %10.4e    %10.4e    %10.4e" % (v, Cis[i], Cvs[i], Sis[i], Svs[i], Nis[i], Nvs[i], ris[i], rvs[i], DLis[i], DLvs[i], Gas[i], DFs[i])
```

Graph

```python
f1 = plt.figure()
plt.plot(t, Cvs, 'r-', label='Cv')
plt.plot(t, Cis, 'b-', label='Ci')
plt.plot(t, Gas, 'g-', label='Growth')
plt.plot(t, DFs, 'c-', label='DF')
plt.grid()
plt.legend(loc='best')
plt.xlabel('time')
plt.xscale('log')
#p.xlim(1e-2, 1e10)
plt.ylabel('population')
plt.yscale('log')
#p.ylim(1e-8, 1e1)
plt.title('Evolution of Cv and Ci')
f1.savefig('hexagon121(Single Crystal).png')
raw_input()
```

8.2 Polycrystalline python code structure

```python
import math as m
from numpy import *
from scipy.integrate import odeint
import matplotlib.pyplot as plt
plt.ion()



## Constant
TWO_PI = 2. * pi



## Parameter setting
# Model parameter, ODE 계산중 변화하지 않음

K0 = 4.3e15              # 1/s/cm3, Defect Generation
Kiv = 1.256e-12          # cm2/s, Interstitial and Vacancy Recombination
Dv = 3.e-17              # cm2/s, Vacancy Diffusion Coefficient
Di = 8.e-6               # cm2/s, Interstitial Diffusion Coefficient
DLp = 20.e9              # 1/cm2, Initial Disloction line Density at Prism Plane
DLb = 5.e9               # 1/cm2, Initial Disloction line Density at Basal Plane
BV = 3.23e-8             # cm, Bugers Vector
GB = 5e-4                # cm, Grain Boundary Diameter
F = 0.1                  # Constant, Texture
G = 1 - 3*F              # Constant, Anisotropy Factor
Zvdp = 1.                # Constant, Bias Factor at Dislocation line in Prism Plane
Zidp = 1.56              # Constant, Bias Factor at Dislocation line in Prism Plane
Zvdlp = 1.               # Constant, Bias Factor at Dislocation loop in Prism Plane
Zidlp = 1.               # Constant, Bias Factor at Dislocation loop in Prism Plane
Zvdb = 1.                # Constant, Bias Factor at Dislocation line in Basal Plane
Zidb = 0.586             # Constant, Bias Factor at Dislocation line in Basal Plane
Zvdlb = 1.               # Constant, Bias Factor at Dislocation loop in Basal Plane
Zidlb = 0.586            # Constant, Bias Factor at Dislocation loop in Basal Plane
Zvgp = 1.                # Constant, Bias Factor at Grain Boundary in Prism Plain
Zigp = 1.56              # Constant, Bias Factor at Grain Boundary in Prism Plain
```

Zvgb = 1.   # Constant, Bias Factor at Grain Boundary in Basal Plain
Zigb = 0.586   # Constant, Bias Factor at Grain Boundary in Basal Plain

Model2,
def dF_dt2(C, t=0):
    """ Return the growth rate of Cv and Ci. """
    Cv, Ci, Si, Sv, Ni, Nv, ri, rv, DLi, DLv, kg, dpa, Ga, DF1, DF2, DF3 = C

    # dpa relation with time
    ddpa_dt = 1e-7

    # <a> Loop Number Density in Prism Plane
    if 0. <= dpa <= 3.5:
        dNi_dt = 0. # 1/cm3/s
    else:
        dNi_dt = 0. # 1/cm3/s

    # <c> Loop Number Density in Basal Plane
    if 0. <= dpa <= 3.0:
        dNv_dt = 0. # 1/cm3/s
    else:
        dNv_dt = 0. # 1/cm3/s

    # <a> Loop Ridius
    dri_dt = sqrt(Si / (pi * BV * Ni)) - ri
    ri = sqrt(Si / (pi * BV * Ni))   # cm

    # <c> Loop Ridius
    drv_dt = sqrt(Sv / (pi * BV * Nv)) - rv
    rv = sqrt(Sv / (pi * BV * Nv))   # cm

    # <a> Loop Defect Number

```python
dSi_dt = TWO_PI * ri * Ni * (Di * Ci / (4.3e22) - Dv * Cv / (4.3e22))      # 1/s
if 0 <= dSi_dt:
    dSi_dt = dSi_dt
else:
    dSi_dt = 0.



# <c> Loop Defect Number
dSv_dt = TWO_PI * rv * Nv * (Zvdb * Dv * Cv / (4.3e22) - Zvdb * Di * Ci / (4.3e22))     # 1/s
if dSv_dt <= 0.:
    dSv_dt = 0.
else:
    dSv_dt = 0.


# <a> Loop Density
dDLi_dt = TWO_PI * ri * Ni - DLi
DLi = TWO_PI * ri * Ni      # 1/cm2,



# <c> Loop Density
dDLv_dt = TWO_PI * rv * Nv - DLv
DLv = TWO_PI * rv * Nv      # 1/cm2,



# Dislocatio Line & Loop Denstiy
TDp = DLp + DLi             # 1/cm2, Total Dislocation Density in Prism plane
TDb = DLb + DLv             # 1/cm2, Total Dislocation Density in basal plane
TD = TDp + TDb              # 1/cm2, Total Dislocation Density



# Grain boundary sink strength
dkg_dt = 0#6 * sqrt(TD)/GB - kg
kg = 2.4e9#6 * sqrt(TD)/GB          # 1/cm2, Bullough model



# Defect Concentration in Cubic per cm3
```

```
        dCv_dt = K0 - Kiv*Ci*Cv - Zvdlp*Dv*Cv*DLi - Zvdp*Dv*Cv*DLp - Zvdlb*Dv*Cv*DLv -
Zvdb*Dv*Cv*DLb - 0.5*Zvgp*kg*Cv*Dv - 0.5*Zvgb*kg*Cv*Dv    # cm3/s
        dCi_dt = K0 - Kiv*Ci*Cv - Zidlp*Di*Ci*DLi - Zidp*Di*Ci*DLp - Zvdlb*Di*Ci*DLv -
Zidb*Di*Ci*DLb - 0.5*Zigp*kg*Ci*Di - 0.5*Zvgb*kg*Ci*Di    # cm3/s



        # Defect Fflux
        Idf = (Di * Ci / (4.3e22))
        Vdf = (Dv * Cv / (4.3e22))



        # Growth stain
        dGa_dt   =   G*0.5*DLp*(Zidp*Idf-Zvdp*Vdf)   +   G*0.5*DLi*(Zidlp*Idf-Zvdlp*Vdf)   +
0.5*kg*(Zigp*Idf-Zvgp*Vdf)    # 1/s



        # Defect Flux
        dDF1_dt = Di * dCi_dt/(4.3e22) - Dv * dCv_dt/(4.3e22)                        # 1/cm/s
        dDF2_dt = Zidp * Di * dCi_dt/(4.3e22) - Zvdp * Dv * dCv_dt/(4.3e22)          # 1/cm/s
        dDF3_dt = Zigb * Di * dCi_dt/(4.3e22) - Zvgb * Dv * dCv_dt/(4.3e22)          # 1/cm/s



        return dCv_dt, dCi_dt, dSi_dt, dSv_dt, dNi_dt, dNv_dt, dri_dt, drv_dt, dDLi_dt, dDLv_dt, dkg_dt,
ddpa_dt, dGa_dt, dDF1_dt, dDF2_dt, dDF3_dt



t = []
exponent_start = -7
exponent_stop = 9
for exponent in range(exponent_start, exponent_stop):
    for mantissa in arange(1, 10, 0.25):
        t.append(mantissa * 10 ** exponent)
t.append(1. * 10 ** exponent_stop)
t = array(t)


## Model2 Integration
```

```python
# Initial value for Model2
C0 = array([1e-10,       # Cv0
            1e-10,       # Ci0
            1e-10,       # Si0
            1e-10,       # Sv0
            1e-4,        # Ni0
            1e-4,        # Nv0
            1e-20,       # ri0
            1e-20,       # rv0
            1e-10,       # DLi0
            1e-10,       # DLv0
            2.4e9,       # kg0
            0,           # dpa0
            0,           # dGa0
            0,           # DF10
            0,           # DF20
            0])          # DF30
```

```python
# Integration for Model2
C, infodict = odeint(dF_dt2, C0, t, full_output=True)
print infodict['message']
```

```python
## Data resolve
Cvs = C[:,0]
Cis = C[:,1]
Sis = C[:,2]
Svs = C[:,3]
Nis = C[:,4]
Nvs = C[:,5]
ris = C[:,6]
rvs = C[:,7]
DLis = C[:,8]
DLvs = C[:,9]
kgs = C[:,10]
```

```
dpas = C[:,11]
Gas = C[:,12]
DF1s = C[:,13]
DF2s = C[:,14]
DF3s = C[:,15]


## Data print
print "%-10s   %-10s   %-10s   %-10s   %-10s   %-10s   %-10s   %-10s   %-10s   %-10s   %-10s   %-10s   %-10s   %-10s   %-10s   %-10s" % ("dpa", "Cvs", "Cis", "Sis", "Svs", "Nis", "Nvs", "ris", "rvs", "DLis", "DLvs", "kgs", "Gas", "DF1s", "DF2s", "DF3s")
print 5 * "=============================="
for i, v in enumerate(dpas):
    print
"%10.4e   %10.4e   %10.4e   %10.4e   %10.4e   %10.4e   %10.4e   %10.4e   %10.4e   %10.4e   %10.4e   %10.4e   %10.4e   %10.4e   %10.4e   %10.4e" % (v, Cvs[i], Cis[i], Sis[i], Svs[i], Nis[i], Nvs[i], ris[i], rvs[i], DLis[i], DLvs[i], kgs[i], Gas[i], DF1s[i], DF2s[i], DF3s[i])


## Graph
f1 = plt.figure()
plt.plot(t, Cvs, 'r-', label='Cv')
plt.plot(t, Cis, 'b-', label='Ci')
plt.plot(t, Gas, 'g-', label='Growth')
plt.plot(t, DF1s, 'c-', label='DF1')
plt.plot(t, DF2s, 'r-', label='DF2')
plt.plot(t, DF3s, 'y-', label='DF3')
plt.grid()
plt.legend(loc='best')
plt.xlabel('time')
plt.xscale('log')
#p.xlim(1e-2, 1e10)
plt.ylabel('population')
plt.yscale('log')
#p.ylim(-1e-8, 1e1)
plt.title('Evolution of Cv and Ci')
```

```
f1.savefig('hexagon122(Cold Worked).png')
raw_input()
```

ANSYS®

IX. Project

First Saved	Monday, April 01, 2013
Last Saved	Monday, December 30, 2013
Product Version	13.0 Release
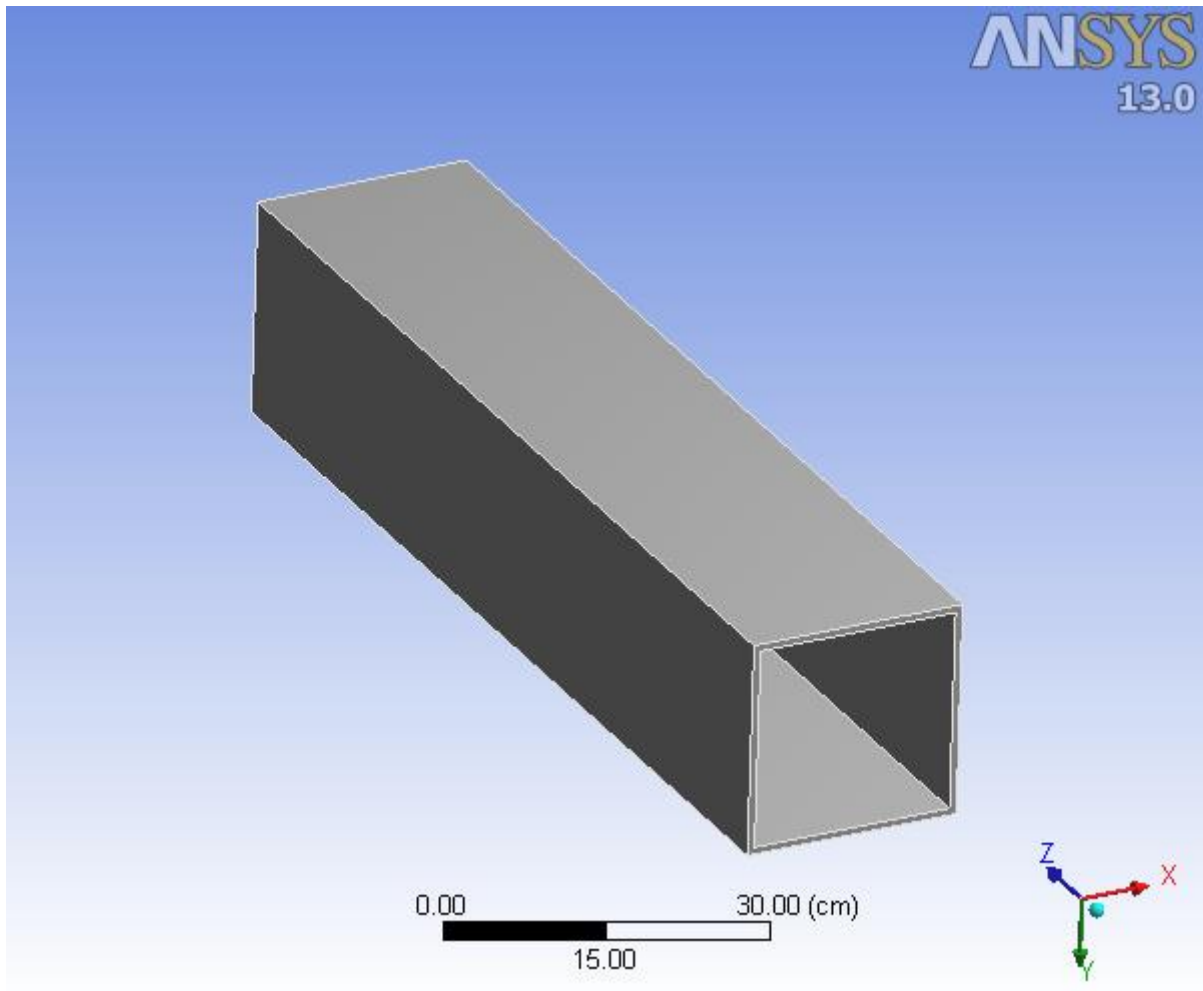
Contents

Units

TABLE 1

Unit System	Metric (cm, g, dyne, s, V, A) Degrees rad/s Celsius
Angle	Degrees
Rotational Velocity	rad/s
Temperature	Celsius

Model (B4)

Geometry

TABLE 2
Model (B4) > Geometry

Object Name	*Geometry*
State	Fully Defined
Definition	
Source	C:\Users\CSI\Desktop\zircaloy-4 구조재 조사성장 FEM medel\zircaloy-4(guide structure)-1_files\dp0\SYS\DM\SYS.agdb
Type	DesignModeler
Length Unit	Millimeters
Element Control	Program Controlled
Display Style	Part Color
Bounding Box	
Length X	21.4 cm
Length Y	21.4 cm
Length Z	100. cm
Properties	

Volume	5796. cm³
Mass	45499 g
Scale Factor Value	1.
Statistics	
Bodies	1
Active Bodies	1
Nodes	8208
Elements	1440
Mesh Metric	None
Preferences	
Parameter Processing	Yes
Personal Parameter Key	DS
CAD Attribute Transfer	No
Named Selection Processing	No
Material Properties Transfer	No
CAD Associativity	Yes
Import Coordinate Systems	No
Reader Save Part File	No
Import Using Instances	Yes
Do Smart Update	No
Attach File Via Temp File	Yes
Temporary Directory	C:\Users\CSI\AppData\Local\Temp
Analysis Type	3-D
Enclosure and Symmetry Processing	Yes

TABLE 3
Model (B4) > Geometry > Parts

Object Name	*Solid*
State	Meshed
Graphics Properties	
Visible	Yes
Transparency	1
Definition	
Suppressed	No
Stiffness Behavior	Flexible
Coordinate System	Default Coordinate System
Reference Temperature	By Environment
Material	
Assignment	Structural Steel
Nonlinear Effects	Yes
Thermal Strain Effects	Yes
Bounding Box	
Length X	21.4 cm
Length Y	21.4 cm
Length Z	100. cm
Properties	

Volume	5796. cm³
Mass	45499 g
Centroid X	-3.4279e-016 cm
Centroid Y	-4.2849e-016 cm
Centroid Z	50. cm
Moment of Inertia Ip1	4.1168e+007 g·cm²
Moment of Inertia Ip2	4.1168e+007 g·cm²
Moment of Inertia Ip3	6.506e+006 g·cm²
Statistics	
Nodes	8208
Elements	1440
Mesh Metric	None

Coordinate Systems

TABLE 4
Model (B4) > Coordinate Systems > Coordinate System

Object Name	*Global Coordinate System*
State	Fully Defined
Definition	
Type	Cartesian
Coordinate System ID	0.
Origin	
Origin X	0. cm
Origin Y	0. cm
Origin Z	0. cm
Directional Vectors	
X Axis Data	[1. 0. 0.]
Y Axis Data	[0. 1. 0.]
Z Axis Data	[0. 0. 1.]

Mesh

TABLE 5
Model (B4) > Mesh

Object Name	*Mesh*
State	Solved
Defaults	
Physics Preference	Mechanical
Solver Preference	Mechanical APDL
Relevance	0
Sizing	
Use Advanced Size Function	Off
Relevance Center	Coarse
Element Size	Default
Initial Size Seed	Active Assembly
Smoothing	Medium
Transition	Fast
Span Angle Center	Coarse
Minimum Edge Length	20.0 cm
Inflation	

Use Automatic Inflation	None
Inflation Option	Smooth Transition
Transition Ratio	0.272
Maximum Layers	5
Growth Rate	1.2
Inflation Algorithm	Pre
View Advanced Options	No
Advanced	
Shape Checking	Standard Mechanical
Element Midside Nodes	Program Controlled
Straight Sided Elements	No
Number of Retries	Default (4)
Extra Retries For Assembly	Yes
Rigid Body Behavior	Dimensionally Reduced
Mesh Morphing	Disabled
Defeaturing	
Pinch Tolerance	Please Define
Generate Pinch on Refresh	No
Automatic Mesh Based Defeaturing	On
Defeaturing Tolerance	Default
Statistics	
Nodes	8208
Elements	1440
Mesh Metric	None

TABLE 6
Model (B4) > Mesh > Mesh Controls

Object Name	*Mapped Face Meshing*
State	Fully Defined
Scope	
Scoping Method	Geometry Selection
Geometry	2 Faces
Definition	
Suppressed	No
Constrain Boundary	No
Advanced	
Specified Sides	No Selection
Specified Corners	No Selection
Specified Ends	No Selection

Transient (B5)

TABLE 7
Model (B4) > Analysis

Object Name	*Transient (B5)*
State	Solved
Definition	
Physics Type	Structural
Analysis Type	Transient
Solver Target	Mechanical APDL
Options	

Environment Temperature	22. °C
Generate Input Only	No

TABLE 8
Model (B4) > Transient (B5) > Initial Conditions

| Object Name	Initial Conditions
State	Fully Defined

TABLE 9
Model (B4) > Transient (B5) > Analysis Settings

Object Name	Analysis Settings
State	Fully Defined
Step Controls	
Number Of Steps	1.
Current Step Number	1.
Step End Time	1. s
Auto Time Stepping	On
Define By	Time
Initial Time Step	1. s
Minimum Time Step	1. s
Maximum Time Step	10. s
Time Integration	On
Solver Controls	
Solver Type	Program Controlled
Weak Springs	Program Controlled
Large Deflection	On
Restart Controls	
Generate Restart Points	Program Controlled
Retain Files After Full Solve	No
Nonlinear Controls	
Force Convergence	Program Controlled
Moment Convergence	Program Controlled
Displacement Convergence	Program Controlled
Rotation Convergence	Program Controlled
Line Search	Program Controlled
Stabilization	Off
Output Controls	
Calculate Stress	Yes
Calculate Strain	Yes
Calculate Contact	No
Calculate Results At	All Time Points
Damping Controls	
Beta Damping Define By	Direct Input
Beta Damping Value	0.
Numerical Damping	0.1
Analysis Data Management	

Solver Files Directory	C:\Users\CSI\Desktop\zircaloy-4 구조재 조사성장 FEM medel\zircaloy-4(guide structure)-1_files\dp0\SYS-1\MECH\
Future Analysis	None
Scratch Solver Files Directory	
Save MAPDL db	No
Delete Unneeded Files	Yes
Nonlinear Solution	Yes
Solver Units	Active System
Solver Unit System	cgs

TABLE 10
Model (B4) > Transient (B5) > Loads

Object Name	*Displacement*	*Thermal Condition*	*Fixed Support*
State	Suppressed	Fully Defined	
Scope			
Scoping Method	Geometry Selection		
Geometry	4 Faces	1 Body	2 Faces
Definition			
Type	Displacement	Thermal Condition	Fixed Support
Define By	Components		
Coordinate System	Global Coordinate System		
X Component	Free		
Y Component	Free		
Z Component	Free		
Suppressed	Yes	No	
Magnitude		Tabular Data	
Tabular Data			
Independent Variable		Z	
Coordinate System		Global Coordinate System	
Graph Controls			
X-Axis		Z	

FIGURE 1
Model (B4) > Transient (B5) > Thermal Condition
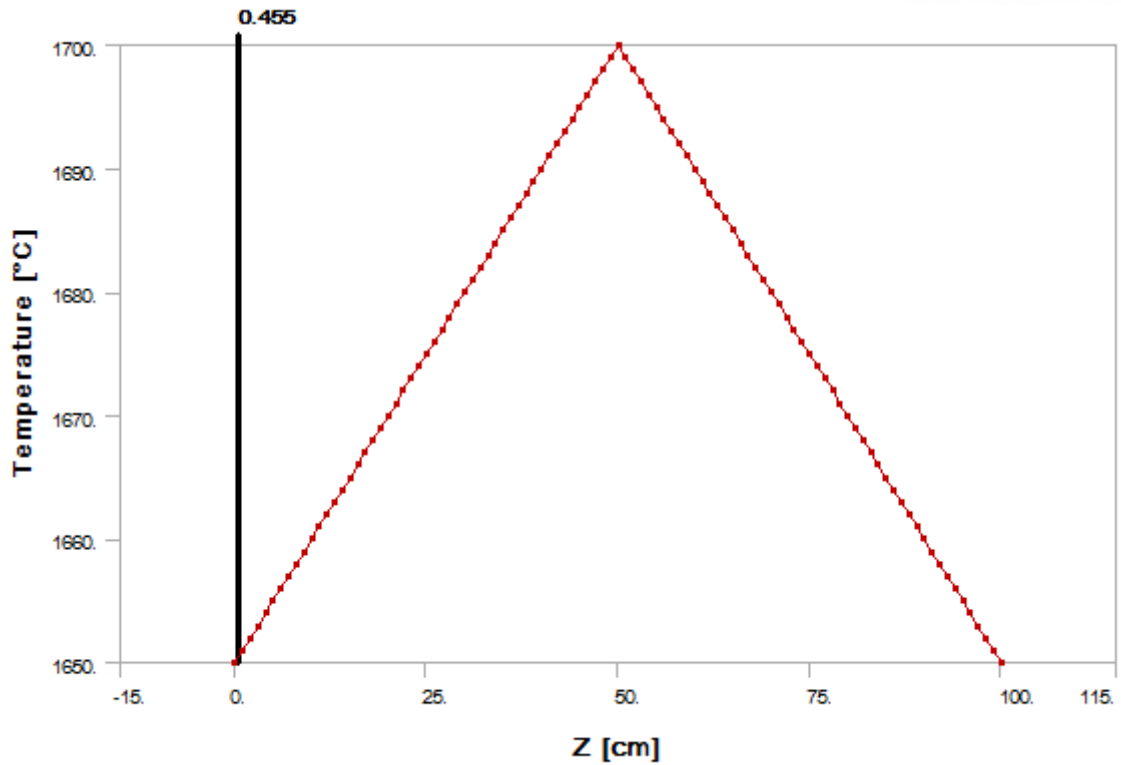
Solution (B6)

TABLE 12
Model (B4) > Transient (B5) > Solution

Object Name	Solution (B6)
State	Solved
Adaptive Mesh Refinement	
Max Refinement Loops	1.
Refinement Depth	2.
Information	
Status	Done

TABLE 13
Model (B4) > Transient (B5) > Solution (B6) > Solution Information

Object Name	Solution Information
State	Solved
Solution Information	
Solution Output	Solver Output
Newton-Raphson Residuals	0
Update Interval	2.5 s
Display Points	All

TABLE 14
Model (B4) > Transient (B5) > Solution (B6) > Results

Object Name	Equivalent Elastic Strain	Equivalent Stress
State	Solved	
Scope		
Scoping Method	Geometry Selection	

101

Geometry	All Bodies	
Definition		
Type	Equivalent (von-Mises) Elastic Strain	Equivalent (von-Mises) Stress
By	Time	
Display Time	Last	
Calculate Time History	Yes	
Identifier		
Integration Point Results		
Display Option	Averaged	
Results		
Minimum	5.3655e-003 cm/cm	1.0731e+010 dyne/cm²
Maximum	1.3809e-002 cm/cm	2.7617e+010 dyne/cm²
Information		
Time	1. s	
Load Step	1	
Substep	1	
Iteration Number	15	

Material Data

Structural Steel

TABLE 15
Structural Steel > Constants

Density	7.85 g cm^-3
Specific Heat	4.34e+006 erg g^-1 C^-1
Thermal Conductivity	0.605 W cm^-1 C^-1
Resistivity	1.7e-005 ohm cm

TABLE 16
Structural Steel > Compressive Ultimate Strength

Compressive Ultimate Strength dyne cm^-2
0

TABLE 17
Structural Steel > Compressive Yield Strength

Compressive Yield Strength dyne cm^-2
2.5e+009

TABLE 18
Structural Steel > Tensile Yield Strength

Tensile Yield Strength dyne cm^-2
2.5e+009

TABLE 19
Structural Steel > Tensile Ultimate Strength

Tensile Ultimate Strength dyne cm^-2
4.6e+009

TABLE 20
Structural Steel > Orthotropic Instantaneous Coefficient of Thermal Expansion

Temperature C	Coefficient of Thermal Expansion X direction C^-1	Coefficient of Thermal Expansion Y direction C^-1	Coefficient of Thermal Expansion Z direction C^-1
	0	0	5.e-006

TABLE 21
Structural Steel > Alternating Stress Mean Stress

Alternating Stress dyne cm^-2	Cycles	Mean Stress dyne cm^-2
3.999e+010	10	0
2.827e+010	20	0
1.896e+010	50	0
1.413e+010	100	0
1.069e+010	200	0
4.41e+009	2000	0
2.62e+009	10000	0
2.14e+009	20000	0
1.38e+009	1.e+005	0
1.14e+009	2.e+005	0
8.62e+008	1.e+006	0

TABLE 22
Structural Steel > Strain-Life Parameters

Strength Coefficient dyne cm^-2	Strength Exponent	Ductility Coefficient	Ductility Exponent	Cyclic Strength Coefficient dyne cm^-2	Cyclic Strain Hardening Exponent
9.2e+009	-0.106	0.213	-0.47	1.e+010	0.2

TABLE 23
Structural Steel > Isotropic Elasticity

Temperature C	Young's Modulus dyne cm^-2	Poisson's Ratio	Bulk Modulus dyne cm^-2	Shear Modulus dyne cm^-2
	2.e+012	0.3	1.6667e+012	7.6923e+011

TABLE 24
Structural Steel > Isotropic Relative Permeability

Relative Permeability
10000